Clinico pathological and molecular characterization of tubulocystic variants of renal tumors

Skenderi, Faruk

UNIVERSITY OF ZAGREB
SCHOOL OF MEDICINE

Faruk Skenderi

Clinico pathological and molecular characterization of tubulocystic variants of renal tumors

DISSERTATION

Zagreb, 2021

UNIVERSITY OF ZAGREB
SCHOOL OF MEDICINE

Faruk Skenderi

Clinico pathological and molecular characterization of tubulocystic variants of renal tumors

DISSERTATION

Zagreb, 2021

This PhD thesis has been completed at the Department of Pathology, Clinical Center University of Sarajevo, Bosnia and Herzegovina, Department of Pathology and Cytology Ljudevit Jurak, University Clinical Hospital Sestre Milosrdnice, Zagreb, Croatia, and Department of Pathology, Faculty of Medicine in Plzen, Charles University in Prague, Czech Republic. The supervisors of the thesis were Professors Monika Ulamec, MD, PhD, and Semir Vranić, MD, PhD.

Parts of this thesis were published in:

1. **Skenderi F,** Ulamec M, Vranic S, Bilalovic N, Peckova K, Rotterova P, et al. Cystic Renal Oncocytoma and Tubulocystic Renal Cell Carcinoma: Morphologic and Immunohistochemical Comparative Study. Appl Immunohistochem Mol Morphol. 2016;24(2):112-9.
2. Ulamec M, **Skenderi F**, Zhou M, Kruslin B, Martinek P, Grossmann P, et al. Molecular Genetic Alterations in Renal Cell Carcinomas With Tubulocystic Pattern: Tubulocystic Renal Cell Carcinoma, Tubulocystic Renal Cell Carcinoma With Heterogenous Component and Familial Leiomyomatosis-associated Renal Cell Carcinoma. Clinicopathologic and Molecular Genetic Analysis of 15 Cases. Appl Immunohistochem Mol Morphol. 2016;24(7):521-30.
3. Peckova K, Martinek P, Pivovarcikova K, Vanecek T, Alaghehbandan R, Prochazkova K, Montiel DP, Hora M, **Skenderi F,** Ulamec M, Rotterova P, Daum O, Ferda J, Davidson W, Ondic O, Dubova M, Michal M, Hes O. Cystic and necrotic papillary renal cell carcinoma: prognosis, morphology, immunohistochemical, and molecular-genetic profile of 10 cases. Ann Diagn Pathol. 2017;26:23-30.
4. Foix MP, Dunatov A, Martinek P, Mundó EC, Suster S, Sperga M, Lopez JI, Ulamec M, Bulimbasic S, Montiel DP, Alaghehbandan R, Peckova K, Pivovarcikova K, Ondrej D, Rotterova P, **Skenderi F,** Prochazkova K, Dusek M, Hora M, Michal M, Hes O. Morphological, immunohistochemical, and chromosomal analysis of multicystic chromophobe renal cell carcinoma, an architecturally unusual challenging variant. Virchows Arch. 2016;469(6):669-78.

ACKNOWLEDGEMENTS

I am truly grateful to my mentors, doctors Monika Ulamec and Semir Vranic, who greatly and positively influenced my career and life. Their support and understanding were of crucial importance for the completion of this thesis. I have learned a lot, and still learning from them on our mutual journey in research and experimental pathology.

I am indebted to my true friend, teacher and supporter Dr. Ondrej Hes and his lab, for his unrestricted support, hospitality and sincerity. I am grateful for his openness and endless sense of humor, which made my days during research in Pilsen easy and pleasant.

I am thankful to Dr. Ivan Damjanov, a great, accomplished, and versatile person and pathologist, for his support, encouragement, openness and friendship. It is an honor to be his collaborator on publications, but even more to learn from his immense experience and his professional and academic career.

I am thankful to Dr. Muzafer Mujic for his long-lasting support, kindness, and motivation. He is another of the inspiring persons that influenced my life and career.

I am thankful to my former chief of department, Dr. Nurija Bilalovic, for encouragement and stimulation to pursue my research career.

My special thank-you to my department collegues Dr. Nermina Ibisevic and Dr. Adisa Chikha for their numerous consultations during my training and junior pathologist years. I thank them for their sincere friendship and being my guardian angles in difficult pathology cases.

Finally, I am deeply grateful to my wife Sanela and my children Nejra, Aiša, and Husein-Ali for their patience and understanding for my habitual absence required to complete many of my research, clinical and academic duties.

CONTENTS

ABBREVIATIONS

RCC	Renal cell carcinoma
TCRCC	Tubulocystic Renal cell carcinoma
RO	Renal oncocytoma
cRO	Cystic renal oncocytoma
ChRCC	Chromophobe renal cell carcinoma
cChRCC	Cystic chromophobe renal cell carcinoma
PRCC	Papillary renal cell carcinoma
cPRCC	cystic Papillary renal cell carcinoma
HGRCC	High-grade renal cell carcinoma
VHL	Von Hippel Lindau gene
WHO	World Health Organization
CGH	Comparative genomic hybridization
FISH	Fluorescence in situ hybridization
PCR	Polymerase chain reaction
FFPE	Formalin-fixed paraffin-embedded tissue

1 INTRODUCTION

1.1 Anatomy, histology, and physiology of the kidneys

Kidneys are a pair of bean-shaped organs located in the upper abdominal region, on either side of the spine in the retroperitoneal space, between the parietal peritoneum and the posterior abdominal wall. They are about 10–13 cm in length, 5-6 cm wide, and about 4 cm thick. Each kidney weighs about 120–170 g in males and 110–150 g in females. Kidneys are covered by a fibrous capsule composed of dense connective tissue helping to hold their shape and protect them. This capsule is covered by a layer of adipose tissue known as the renal fat pad, which is then encompassed by a Gerota's fascia. The fascia and the overlying peritoneum serve to tightly hold the kidneys to the posterior abdominal wall in a retroperitoneal position, while adjacent muscles, fat and ribs serve to protect the kidneys from physical injuries (Figure 1 A-B)

The renal hilum is the entry and exit site for vessels, nerves, lymphatics, and ureters. The medial-facing hila are inserted into the convex indentation of the kidney. An anterior section through the kidney shows an outer region called the renal cortex and an inner region called the renal medulla. In the medulla, 5-8 renal pyramids are separated by renal columns. Each pyramid creates urine and ends in a renal papilla. Each renal papilla drains into a collecting structure called a minor calyx. Several minor calyces connect to form a major calyx. All major calyces connect to the single renal pelvis, connecting to the ureter (Figure 1).

Nephrons are the "functional units" of the kidney. They clean the blood of metabolic waste and balance the homeostatic set values by filtration, reabsorption, and

secretion. They are also involved in blood pressure control through the renin, red blood cell production through the erythropoietin, and calcium absorption through the conversion of calcidiol into calcitriol, the active form of vitamin D. Nephron consists of the renal corpuscle, proximal convoluted tubules (PCT), loop of Henle, and distal convoluted tubules (DCT). The glomerulus is a capillary bed that filters blood mainly based on particle size. The filtrate is captured by Bowman's capsule and then moves through the PCT, the loop of Henle and DCT, where absorption and secretion of several substances occur (1).

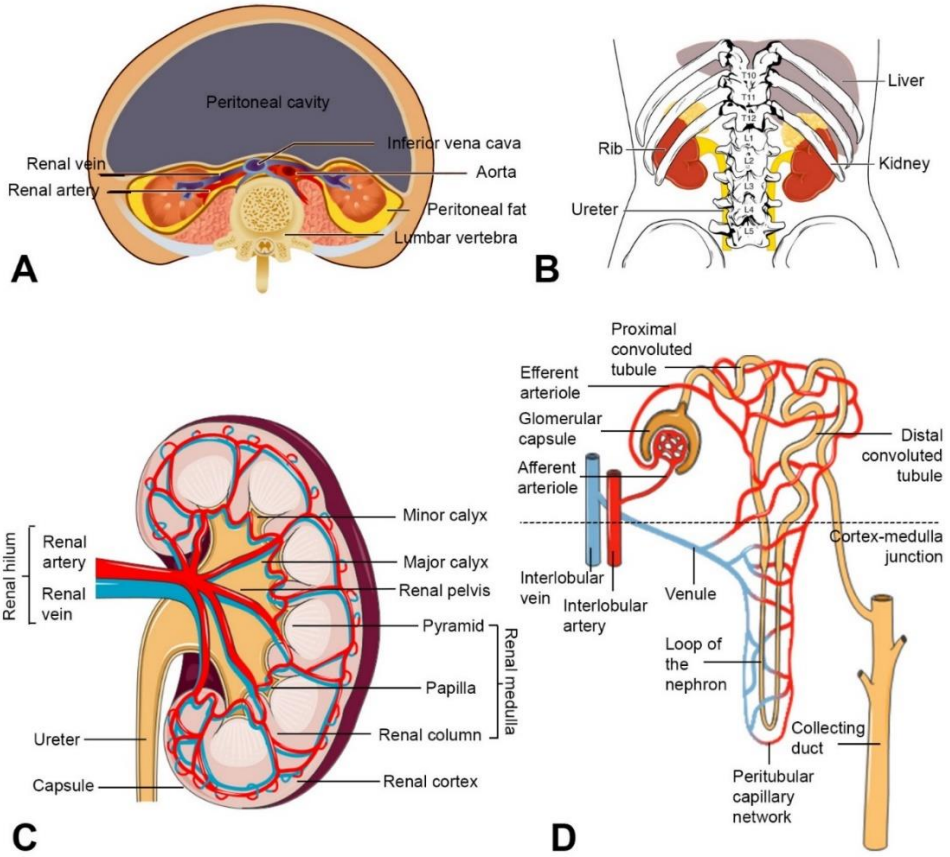

Figure 1. Location and anatomy of the kidneys. (A) Transversal view of the kidneys location and relationship to adjacent organs. (B) Posterior view of the kidneys location and relationship to adjacent organs. (C) The anterior section of the kidney with the internal anatomy review. (D) The anatomy of the nephron, the functional unit of the kidney. (Illustrations are adapted based on Creative Commons license 4.0)

Histologically, the kidney is composed of closely packed proximal and distal convoluted tubules, tubules of the loop of Henle, collecting ducts, small blood vessels, and interspersed renal corpuscula. The renal corpuscle comprises a bed of capillaries called the glomerulus, and the associated cells and structures, known as the podocytes and the intraglomerular mesangial cells. Glomeruli are contained within the Bowman capsule. The lighter space between these two is called the Bowman space. PCT is lined by simple cuboidal epithelium, and cells are eosinophilic with numerous mitochondria, prominent basal folds, and lateral interdigitations, containing long microvilli, and with lumens often occluded (2). The distal tubules are lined by simple cuboidal epithelium with cells smaller than in PCT, with short microvilli faint or clear cytoplasm and more empty lumens (3). Collecting ducts are lined by cuboidal to columnar, pale-staining cells with distinct cell membranes (Figure 2).

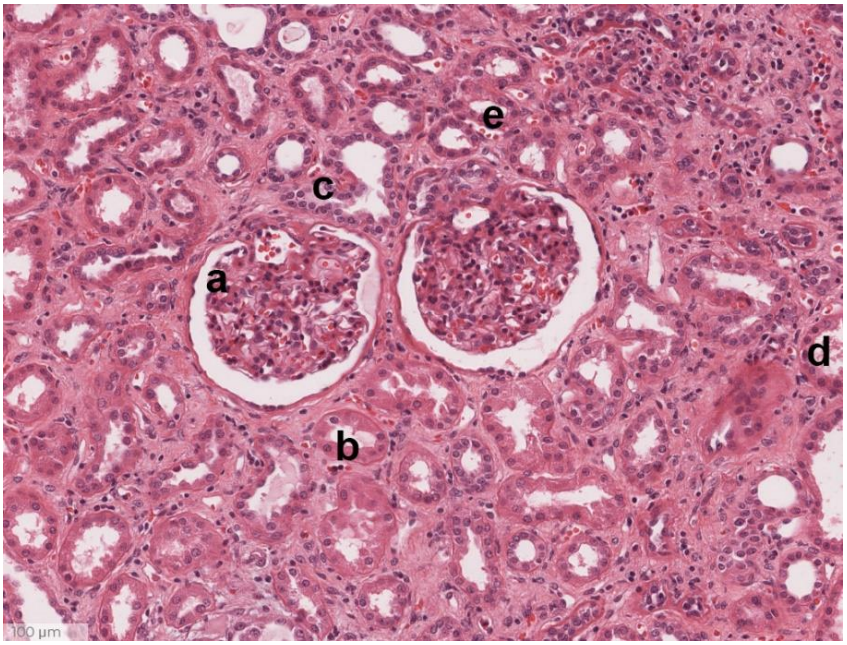

Figure 2. Normal kidney histology showing the glomerulus (a), proximal convoluted tubule (b), distal convoluted tubule (c), collecting duct (d), and capillary blood vessels (e).

1.2 Renal tumors

1.2.1 Epidemiology, etiology, and pathogenesis

Renal tumors are a heterogeneous group of neoplasms showing a variety of histological and genetic features. They account for 5% and 3% of all malignancies, and they are the 9th and 14th most common cancers in men and women, respectively (4, 5). The incidence of Renal cell carcinoma (RCC) varies from region to region. About 70% of cases occur in developed countries, with the highest rates in the Czech Republic and North America and the lowest in Africa and Eastern Asia (6, 7). RCC is more frequent in men than in women, with a ratio of about 2:1. It occurs mostly in the sixth to eighth decade of life, while it is unusual in patients aged under 40 years and is rare in children. The incidence increased over the last decades, but the current trends show stagnation in certain countries (8).

Renal cell tumors are the 16th most common cause of death from cancer worldwide (7). The five-year survival rate has doubled over the last 60 years, mostly due to earlier detection at smaller sizes and effective surgical treatment (9).

RCC etiology has been associated with several risk factors, of which many are also common to other cancer types, such as obesity, cigarette smoking, and occupational exposure to toxins (7, 10). In contrast, others are more specific for kidney tumors, such as hypertension, acquired cystic kidney disease, end-stage kidney disease, hemodialysis, kidney transplantation, or tuberous sclerosis syndrome (5, 11, 12). Most RCCs are sporadic; nevertheless, hereditary genetic factors are responsible for RCCs in 2-4% of cases. Several syndromes with a distinct genetic basis and phenotype are described, the

most common one being Von Hippel Lindau (VHL) disease (4, 11). Factors that may indicate a hereditary role in patients without clear genetic disease include first-degree relatives with a tumor, onset before the age of 40, and bilateral or multifocal disease (13). Inherited polycystic disease increases the risk for RCC. Additional factors that may increase the risk for RCC include cytotoxic chemotherapy, chronic hepatitis C infection, sickle cell disease, and kidney stones (14-16).

Pathogenesis of any neoplastic process is based on genetic abnormalities, and RCCs are no exception in this regard. Some genetic abnormalities are frequently encountered in a particular tumor type, such as *VHL* mutation or hypermethylation and chromosome 3p loss in clear cell RCC. A variety of other genetic abnormalities are observed across the spectrum of renal neoplasia, including gene mutations, amplifications, rearrangements, and others. Some genetic alterations are typical, thus defining a distinctive molecular tumor type, such as Succinate dehydrogenase-deficient renal cell carcinoma (SDRCC), or MiT family translocation renal cell carcinomas, or emerging entities, such as Fumarate dehydrogenase deficient RCC (17). Genetic alterations of the selected tumor types will be discussed later.

1.2.2 Classification, histopathological, immunohistochemical, and genetic properties

Renal tumor classification underwent a significant evolution since its early forms published in 1975 by the Armed Forces Institute of Pathology (AFIP) in the United States, or the first World Health Organization (WHO) classification published in 1981. In these early classifications, renal tumors were grouped into two major categories: Clear cell carcinoma and granular cell carcinoma (11), or renal cell carcinoma, and others (18). In

the following time, the accumulation of research data brought the Mainz classification in 1986, the Heidelberg-Rochester classification in 1997 (18), followed by the WHO classification in 1998, in which today's traditional and major renal tumor subtypes were established. In 2004 the WHO classification was updated and further refined.

In 2016 the WHO published the latest update to their kidney tumor classification with epithelial cell tumors comprising 14 malignant and two benign tumor types (19) (Table 1). The histological criteria remained the foundation for this classification. However, the nomenclature is based on multiple criteria, including cytoplasmic appearance, architecture, a combination of morphologies, anatomic location, underlying disease, familial syndromes, and specific genetic alterations (20). The recent expansion of molecular methods allowed for more profound insight into the genetics of renal tumors, revealing clinically and potentially therapeutically relevant molecular differences within the histological types.

The 2016 WHO classification was preceded by the consensus conference of the International Society of Urological Pathology (ISUP) held in 2012 in Vancouver (Canada). The reports published from the consensus conference were referred to as the 2012 ISUP Vancouver classification of renal neoplasia (21). The ISUP Vancouver classification confirmed the most frequent and well-established tumor subtypes, namely the clear cell renal cell carcinoma (ccRCC), representing 70-80% of all the renal tumors, papillary renal cell carcinoma (PRCC), occurring in 10-15% of the cases, and the chromophobe renal cell carcinoma (ChRCC), in about 5% of cases, as well as other, well established but less frequently occurring tumors (all together in about 10% of the cases). This classification embraced several newly recognized renal cell carcinoma (RCC) subtypes, subsequently included in the 2016 WHO classification. Novel subtypes include

tubulocystic renal cell carcinoma (TCRCC), acquired cystic disease-associated RCC, clear cell papillary RCC, microphthalmia transcription factor-family translocation RCC (including t(6;11) RCC and Xp11.2/TFE3 RCC), hereditary leiomyomatosis RCC syndrome-associated RCC, and succinate dehydrogenase (SDH)-deficient renal carcinoma. Recently, additional emerging entities were reported, including thyroid-like follicular RCC, anaplastic lymphoma kinase translocation RCC, RCC with smooth muscle stroma, eosinophilic, solid, and cystic RCC, and biphasic squamoid alveolar RCC (22-25).

Table 1. WHO Classification of the renal cell tumors published in 2016

Renal cell tumors	**WHO ICO-3 code/behavior**
Clear cell renal cell carcinoma	8310/3
Multilocular cystic renal neoplasm of low malignant potential	8316/1
Papillary renal cell carcinoma	8260/3
Hereditary leiomyomatosis and renal cell carcinoma-associated renal cell carcinoma	8311/3
Chromophobe renal cell carcinoma	8317/3
Collecting duct carcinoma	8319/3
Renal medullary carcinoma	8510/3
MiT family translocation renal cell carcinomas	8311/3
Succinate dehydrogenase-deficient renal cell carcinoma	NA
Mucinous tubular and spindle cell carcinoma	8480/3
Tubulocystic renal cell carcinoma	8316/3
Acquired cystic disease-associated renal cell carcinoma	8316/3
Clear cell papillary renal cell carcinoma	8323/1
Renal cell carcinoma, unclassified	8312/3
Papillary adenoma	8260/0
Oncocytoma	8290/0

NA – not available

Histopathologically and for the purpose of differential diagnosis, RCCs are put into broad groups of tumors with clear cells or eosinophilic cells or solid tumors and papillary tumors. Each of the tumors has few distinctive morphological characteristics; nevertheless, RCCs overlapping morphology is frequently encountered, and use of immunohistochemistry, and occasionally confirmation with molecular methods, is often required.

Renal oncocytoma is a benign tumor with abundant oncocytic cytoplasm, growing in cords, nests, alveoli, and tubules in a fibrous or myxoid stroma. It may contain degenerative atypia but not papillary growth, clear cells, or necrosis. Besides the typical, small cell variant, oncoblastic, pseudorosettes, and cystic variants are described (26, 27). Immunohistochemically, RO is CD117 and E-cadherin positive, and CK7 and vimentin negative, although CK7 may show characteristic scattered cells positive pattern in less than 5% of the tumor. There are no consistent genetic alterations in this tumor that could be used for diagnostic purposes; however, loss of chromosome 1 and Y, rearrangements of 11q13, deletion of 14 were some of the more commonly reported (28).

Papillary renal cell carcinoma (PRCC) is traditionally divided into type 1 and type 2. However, the type 2 tumors represent a broad group with less strictly defined morphological criteria and worse outcomes than more clearly defined type 1 tumors. Type 1 PRCC have thin papillae lined by a single layer of small amphophilic or basophilic cells with nuclei ISUP grade 1 or 2. Type 2 tumors are more heterogeneous, showing papillae lined by large eosinophilic cells with large nuclei with pseudostratification and high-grade nucleoli (29). Some of the tumors show mixed morphological features and are therefore difficult to classify as type 1 or 2. PRCC is positive for AE1-AE3, CAM5.2, HMWCK. AMACR, vimentin, and CD10. Type 1 PRCC rarely occurs in hereditary

circumstances, with characteristic *MET* gene mutation (29). However, this mutation is not consistently found in sporadic tumors. Additionally, among other less frequent alterations, PRCC shows a gain of chromosome 7 and 17 and loss of Y. Type 2 PRCC are much more genetically diverse, showing a broad spectrum of abnormalities.

ChRCC is typically composed of pale, large, finely granular cells with distinct cytoplasmic membrane or eosinophilic cells, with perinuclear halos and raisinoid nuclei (30). However, mixed morphology may be encountered (31). Nuclear grade does not apply. Typically, these tumors are solid with parenchymal extension and often entrapping tubules. Additionally, nests, broad alveoli, and trabeculae may be seen (11). ChRCC is positive for CK7 and CD117, and negative for CA9. Genomic analyses of ChRCC demonstrated a low somatic mutation rate and identified *TP53* and *PTEN* as the most frequently mutated genes (32, 33). Recent cytogenetic and comparative genomic hybridization confirmed distinct genotype of ChRCC, with multiple chromosomal losses of chromosomes 1, 2, 6, 10, 13, 17, 21, and Y chromosome in the majority of chromophobe RCCs (31).

1.2.3 Prognostic factors and therapy

The data in the Surveillance, Epidemiology and End Results (SEER) database show that about 65% of patients present with localized disease, 17% with disease spread to regional lymph nodes, and about 16% with metastatic disease (34). In patients with RCC who present with localized disease, surgical resection can be curative. Unfortunately, more than one-third of patients with RCC present with either locally advanced and unresectable, or metastatic disease. In addition, tumors that were initially

resected eventually recur. The prognosis for patients with locally advanced or metastatic RCC is generally poor.

The factors that affect prognosis include the stage, pathological characteristics such as tumor type, grade and necrosis, clinical factors, and molecular markers.

Tumor, node, metastasis (TNM) staging system is used to evaluate the anatomic extent of the disease and categorize the prognostic stage groups (35). The stage is the most consistent factor that influences the prognosis of the patients with RCC. Patients with stage I and II have tumors of any size limited to the kidney, and their five-year survival rate ranges from more than 90% for stage I and 75-90% for stage II tumors. For tumors in stage III, survival ranges from 59-70%. Stage III tumors include tumors of any size with the invasion of the pyelocaliceal system, major veins, perinephric tissues, or tumors with regional metastases (N1). Stage IV tumors invade Gerota's fascia or have distant metastases (M1). The survival rate for stage IV tumors is about one year (35).

The histologic type of the tumor is also an important factor affecting the prognosis. Clear cell RCC has the worst prognosis, followed by the chromophobe RCC, followed by papillary RCC type 1, which has the most favorable prognosis (36). Less frequent tumor types such as collecting duct carcinoma, medullary carcinoma, or any histologic type with sarcomatoid or rhabdoid features are more aggressive and associated with shorter survival (37). Histologic grade is another independent prognostic factor. Furhman's grade was most widely used until it evolved into ISUP grade. Grade 1 carcinomas had 89%, grade 2 about 65%, and grade 3 only about 46% five-year disease-free survival (38).

Tumor necrosis is an independent predictor of survival and is integrated into some of the staging and prognostic systems for clear cell RCC and chromophobe RCC (39).

Clinical factors such as performance status, paraneoplastic syndromes such as anemia, fever, weight loss, thrombocytosis, hypercalcemia, or obesity may influence survival. Several prognostic models that include the clinical parameters have been used for some time, and the University of California Los Angeles integrated staging system (UISS), which combines Eastern Cooperative Oncology Group (ECOG), Furhman's grade, and TNM, has been validated (40).

Molecular markers affecting tumor aggressiveness and thus the prognosis, or markers important for the diagnosis of particular RCC subtype include: *VHL* gene mutation or methylation, chromosome 3p loss, and *SETD2*, *BAP1*, *PBRM1* mutations in clear cell RCC; Fumarate hydratase (*FH*) deficiency in papillary RCC type 2; *TFE3* and its fusion partners *NONO*, *GRIPAP1*, *RBMX* and *RBM10* in MIT family translocation RCC; Succinate dehydrogenase deficiency, *TFEB/VEGFA/6p21* amplification, *TCEB1* mutation, *ALK* rearrangements, *TSC2* and *MTOR* mutations and other genetic abnormalities in recognized and emerging renal tumor entities (17).

Treatment of the patients with RCC depends on the extent of the disease at the time of diagnosis, patient's age, and comorbidities. Based on the extent of the disease, RCC is designated as localized (stage I, II, or III) or advanced (stage IV: tumor extending into the ipsilateral adrenal gland, or beyond Gerota's fascia (T4), or metastatic disease (M1). The preferred treatment modality for patients in stages I, II, and III is surgical therapy, which presumes partial or radical nephrectomy. Although up to 30% of tumors

recur, systemic adjuvant therapy has not yet been introduced as a standard clinical protocol. There is no clear evidence of survival benefits for the patients. At the same time, the toxicity confers a substantial risk of side effects.

Nevertheless, the FDA approved sunitinib for adjuvant treatment of high-risk RCC despite the small benefit shown over the placebo (DFS 5.8 vs. 6.6 years) (41). Several other agents were investigated in clinical trials and showed only modest benefit over the placebo in the adjuvant setting. Ongoing studies are investigating the adjuvant immune checkpoint inhibitors treatment following the resection of high-risk RCC. Patients with advanced or metastatic disease are treated with systemic therapy. Some of the approved therapeutic protocols include immune checkpoint inhibitors (PD-1 and PD-L1 inhibitors), CTLA-4, and angiogenic (VEGF) inhibitors. The immune checkpoint inhibitors are recently replacing less preferred treatment options such as interleukin 2 (IL-2) interferon-alpha and other interleukins.

1.2.4 Tubulocystic renal cell carcinoma

TCRCC is a new entity included in the latest WHO classification. About 100 cases of this rare tumor have been reported in the literature (21). TCRCC has a characteristic macroscopic appearance. It is a well-circumscribed, encapsulated, gray-colored tumor with the cut surface showing multiple variable-sized cysts resembling a bubble wrap (42, 43). Histologically, it is composed of well-formed tubules and cysts and a scant fibrotic stroma. Tubules and cysts are lined by a single or more layers of atypical cells with abundant eosinophilic cytoplasm, frequent hobnail appearance, and a high grade, enlarged nuclei with prominent nucleoli (27, 43). Not rarely, these tumors may contain areas with classic PRCC morphology, or the associated PRCC may be found in

the tumor proximity, raising the question of their relationship with the PRCC (44, 45). Less frequently, small foci of high-grade RCC may be associated with TCRCC (46). Although the clinical and pathological evidence warrants TRRCC a separate place in the kidney tumor classification, many questions remain unclear, requiring further investigation of its relations with other tumors, molecular genetic properties, and outcome.

Immunohistochemically, since the low number of cases reported in the literature, these tumors are not well defined, and further research is necessary. Available literature reports positive AMACR, vimentin and PAX8, variable CK7 and CD10, and negative CD117 staining (27, 47).

Molecular and genetic analyses showed gains of 7 and 17 and loss of Y, similar to PRCC (11, 45). However, conflicting data come from different studies, some of them concluding that TCRCC does not show gains of 7 and 17, others conclude it shows loss of 9 and gain of 17, having no relationship to PRCC (47-49). No consistent gene mutations were reported in the literature. The molecular features of TRCC need further elucidation.

1.2.5 Cystic histological variants of conventional renal tumors

The most common renal tumors typically present with solid, papillary, or pseudopapillary appearance. However, it is well known that they occasionally present with cystic, tubular, or pseudocystic patterns to a varying extent (11).

Renal oncocytoma is a benign tumor presenting grossly as a well-circumscribed, solid, yellowish-tan mass, often having a central fibrotic area (7). Histologically it grows

in a solid and nested pattern, with large, round eosinophilic cells containing oval nuclei. Stroma is loose and present only in areas with nested architecture. Rarely, this benign tumor presents with an unusual growth pattern build of tubules and cysts, thus mimicking malignant renal neoplasia with tubulocystic growth pattern, such as TCRCC, thus creating a diagnostic difficulty or a pitfall, particularly on small biopsies.

Another renal tumor that may present with an unusual growth is ChRCC. Chromophobe renal cell carcinoma is characterized by pale cells with prominent cell membranes, wrinkled (resinoid) nuclei with perinuclear halos, and smaller eosinophilic cells. It usually shows solid or solid-alveolar architectural patterns. The two recognized ChRCC morphologic variants are classic and eosinophilic. However, the morphological spectrum is broader, and amongst several described variants (50-52), a multicystic growth pattern is sometimes encountered (30).

PRCC, as indicated by its name, shows the papillary architecture. It has a prominent pseudocapsule, papillae formed by delicate fibrovascular cores that often contain foamy macrophages and psammoma bodies. Traditionally, it is subdivided into type 1 and type 2, based on histology differences, clinical behavior, and outcome. Type 1 PRCC shows papillae covered by cells with nuclei arranged in a single layer on the papillary cores, often with scanty pale cytoplasm. Nevertheless, many exceptions to classical morphological subtypes are reported in the literature, and this area is the subject of intense research (53, 54). Although rarely, PRCC may radiologically and pathologically exhibit cystic appearance (55, 56).

1.3 Significance of cystic/tubulocystic growth pattern in renal tumors

Less frequently, tubulocystic or cystic architectural patterns of common renal tumors may represent a significant diagnostic challenge, leading to misdiagnosis, particularly on a small biopsy. Clear morphologic, immunohistochemical, and molecular criteria would improve the diagnostic accuracy and outcome of the patients. In addition, the prognostic significance of cystic or tubulocystic growth patterns in RCC subtypes is yet unclear and has been recently gaining more attraction (57-60). Recent observations suggest that the predominant cystic or tubulocystic architecture in renal tumors predicts better patient outcomes, and this appears to be true across the tumor subtypes (24, 58, 60-62). Furthermore, in a case of resected multilocular cystic renal cell carcinoma, long-term follow-up studies gathered sufficient evidence that this tumor does not metastasize. Hence, its name was revised, and the tumor was placed into a borderline or low malignant potential category in the 2016 WHO classification (61, 63). Similarly, first long-term follow-up studies on clear cell papillary renal cell carcinoma (ccpRCC) have reported no metastatic disease in these patients, proposing a revision of the tumor name and placing it into a benign category (64, 65).

2 HYPOTHESIS

Based on personal experience and available literature, we hypothesize that renal tumor subtypes or variants with cystic or tubulocystic morphology have similar immunoprofile and genetic abnormalities but a more favorable prognosis than their well-described (characterized) conventional counterparts.

3 AIMS

3.1 General aim

To characterize the morphological features, imunoprofile, and molecular genetic profile of recently recognized tumor entity, namely the TCRCC. In addition, to characterize tubulocystic variants of renal tumors subtypes and determine the most useful morphologic, immunohistochemical, and molecular properties for differentiation of these tumors in diagnostic practice. Furthermore, the characterization will elucidate the biological and clinical significance of cystic and tubulocystic variants compared with their conventional subtypes.

3.2 Specific aims

1. To compare the clinicopathological characteristics (age, gender, size, tumor stage, tumor grade, follow-up, architectural growth patterns, stromal features, cytomorphology, ISUP nucleolar grade, necrosis, and mitotic activity) of tubulocystic renal tumor variants with their conventional counterparts.

2. To compare the immunoprofile of cystic and conventional renal tumors and determine the most appropriate biomarkers for differentiation of these tumors in diagnostic settings.

3. To characterize molecular-genetic properties of the tubulocystic variants of renal tumors and make a comparison among tubulocystic groups as well as their conventional counterparts for identifying potential diagnostic molecular biomarkers or molecules involved in pathogenesis and development of these tumors.

4 MATERIALS AND METHODS

4.1 Case selection and study groups

The cases were searched from the Sikl's Department of Pathology registry, Charles' University, Plzen, Czech Republic, which contains more than 19,000 kidney tumors. The Ethical Committee of the Charles University Medical School Plzen, Czech Republic (411/2015), and Ethical Committee of the University of Zagreb School of medicine, Zagreb, Croatia, approved the study.

Renal oncocytomas (RO) were searched in the registry using the keywords “kidney, oncocytoma”. The search revealed 645 cases. Thirty cases of RO with typical morphology, defined by the WHO (7), i.e., round-to-polygonal cells with finely granular, eosinophilic cytoplasm with round to oval nuclei, were retrieved from the archives and revised.

Cystic renal oncocytoma (CRO) cases were refined from the previous search by using the additional keyword “cystic”. The search revealed 36 cases, which were retrieved from the archives and revised. In addition to previously used selection criteria for RO, tumors with at least 50% of the tubulocystic architecture were selected. A total of 24 cases fulfilled the inclusion criteria (3.7% of 645 available RO). Thirty classical, conventional RO were retrieved from archives as a control group.

TCRCCs have been retrieved from the in-house and consultation files of the same registry. A total of 15 cases were available. TCRCC typically demonstrated well-formed, small to medium-sized tubules and cysts lined by large cells, usually demonstrating abundant eosinophilic cytoplasm. The lining cells showed focal hob-nail

shape with high nuclear grade with prominent nucleoli. Cases were reviewed for inclusion criteria, and the diagnosis was confirmed by immunohistochemistry (IHC).

PRCCs have been searched in the registry with keywords “kidney, papillary”, resulting in 1311 cases. Twenty-seven cases of the conventional, grossly solid, microscopically typical PRCC type 1 were retrieved from archives. According to WHO classification, the morphological criteria of PRCC type 1 are Papillary architecture with delicate fibrovascular cores, often with foamy macrophages and psammoma bodies; papillae covered mostly by cells with scanty cytoplasm and nuclei arranged in a single layer (66).

PRCC with cystic and tubular features (cPRCC) were refined from the previous search using additional keywords “cystic, tubular”. The search revealed 10 cases, which were retrieved from the archives and revised using the morphologic criteria for PRCC, with additional inclusion criteria, that is, at least 50% of the tumor showing cystic or tubular architecture. All the tumors were large cystic lesions encapsulated by a thick, mostly fibrotic tissue and showed necrotic areas in addition to cysts and tubules.

ChRCC was searched in the registry using the keywords “kidney, chromophobe”. The search revealed 733 cases. Twenty cases showing well-defined morphologic criteria according to WHO classification were selected, retrieved, and revised. The inclusion criteria were solid, sheet-like, or nested architecture with incomplete, often hyalinized vascular septa, large pale cells with reticular cytoplasm, prominent cell membranes, wrinkled (resinoid) nuclei with perinuclear halo, and common binucleation.

Cystic ChRCCs (cChRCC) were further refined from the previous search by adding the keywords “cystic”, or “tubular”. Searching resulted in 10 cases, retrieved from the archives, and reviewed for criteria applied for conventional ChRCC and, in addition, at least 50% of cystic or tubular architecture. Diagnoses were supported by immunohistochemistry.

All the cases were reviewed by three pathologists (FS, MU, OH). For each case, 1 to 49 tissue blocks (mean 5.6) were available for review, and 1-2 representative blocks were selected for immunohistochemical and molecular genetic studies. Clinical data, follow-up, and macroscopic descriptions were collected by review of the institutional medical records or by contacting the consulting pathologists from different institutions.

4.2 Conventional light microscopy

The tissue had been fixed in 4% buffered formalin, embedded in paraffin, and 3- to 4-μm-thick sections were cut and stained with hematoxylin and eosin. The sections were evaluated by light microscopy for the following histologic features: visually estimated percentage of cystic, solid, and nested patterns, the epithelial lining of the cysts (single, pseudopapillary, multilayered), presence of papillary protrusions in the cysts, hemorrhage within the cysts or stroma, extent and composition of the stroma, presence of foamy macrophages, cytological features including nuclear ISUP nucleolar grade, nuclear pseudostratification, mitotic activity, and the presence of necrosis. In cases of TC-RCC, the percentage of additional histological patterns was recorded.

4.3 Immunohistochemistry

An immunohistochemical study was performed using the following primary antibodies:

Table 2. Antibodies and clones used in the study

Name	**clone name, type, manufacturer, dilution**
AMACR	13H4, monoclonal, DAKO, Glostrup, Denmark, 1:200
Carbonic anhydrase IX	rhCA9, monoclonal, RD systems, Abingdon, GB, 1:100
Vimentin	D9, monoclonal, NeoMarkers, Westinghouse, CA, 1:1000
OSCAR	OSCAR, monoclonal, Covance-SpinChem, 1:500
PAX-8	polyclonal, Cell Marque, Rocklin, CA, 1:25
Cytokeratin 7	OV-TL12/30, monoclonal, DakoCytomation, 1:200
Cytokeratins AE1-AE3	monoclonal, BioGenex, San Ramon, CA, 1:1000
CD117	CD117, polyclonal; DakoCytomation, Glostrup, Denmark; RTU
EMA	E29, monoclonal; Dako, Carpinteria, CA; 1:1000
CD10	56C6, monoclonal; Novocastra, Newcastle, UK; 1:50
TTF-1	SPT24, monoclonal; Novocastra, 1:400
Anti-mitochondrial antigen	MIA, monoclonal; BioGenex; 1:100
Cathepsin K	monoclonal, 3F9, 1:100; Abcam, Cambridge, UK
TFE3	polyclonal, 1:100; Abcam

Antibodies were visualized using the supersensitive streptavidin-biotin-peroxidase complex (Biogenex).

Appropriate positive controls were employed for all assays. Immunohistochemical staining was recorded negative if no staining, or less than 5% of staining was observed; as weak (+) for staining of up to 25% of tumor cells; moderate (++) for staining 25-50% of tumor cells; and strong (+++) for staining in more than 50% of tumor cells.

4.4 DNA extraction

DNA was extracted from formalin-fixed paraffin-embedded (FFPE) tumor and non-tumor tissues (when available) of each case using QIAsymphony DNA Mini Kit (QIAGEN, Hilden, Germany) on an automated extraction system (QIAsymphony SP, QIAGEN), according to the manufacturer's supplementary protocol for FFPE samples (purification of genomic DNA from FFPE tissue using the QIAamp DNA FFPE Tissue Kit and Deparaffinization Solution). The concentration and purity of isolated DNA were tested using NanoDrop ND1000 (NanoDrop Technologies Inc., Wilmington, DE, USA). DNA integrity was examined by amplifying control genes in multiplex PCR, producing fragments from 100 to 600 base pairs. Only cases with DNA integrity equal to or higher than 400 bp were used for further analysis by aCGH.

4.5 Array comparative genomic hybridization

A CytoChip Focus Constitutional (BlueGnome Ltd., Cambridge, UK) microarray processor was used for analysis. CytoChip Focus Constitutional uses BAC technology and covers 143 regions of known significance with 1-Mb spacing across a genome. Probes were spotted in triplicate. First, 400 ng of gDNA was labeled using the Fluorescent Labeling System (BlueGnome Ltd., Cambridge, UK). The procedure consisted of Cy3 labeling of a test sample and Cy5 labeling of a reference sample. MegaPool Reference DNA of the opposite sex was used as a reference sample (Kreatech Diagnostics, Amsterdam, Netherlands). Each labeled pair was mixed, dried, and hybridized overnight at 47 °C using ArrayIt hybridization cassettes (Arrayit Corporation, CA, USA). Posthybridization washing was done using SSC buffers with increasing

stringency. Dried microarrays were scanned with InnoScan 900 (Innopsys, France) at a resolution of 5 μm.

Scanned images were analyzed and quantified using BlueFuse Multi software (BlueGnome Ltd., Cambridge, UK). BlueFuse Multi uses Bayesian algorithms to generate intensity values for each Cy5 and Cy3 labeled spot on the array according to an appropriate .gal file. The reported changes were browsed and interpreted using BlueFuse Multi as well. Cutoff values were set to a log 2 ratio of −0.193 for loss and 0.170 for gain.

4.6 Fluorescence in Situ Hybridization (FISH)

For each case, a 4-mm-thick section was placed onto a positively charged slide. Hematoxylin–eosin-stained slides were examined for the determination of areas for cell counting. The unstained slide was routinely deparaffinized and incubated in the Target Retrieval Solution Citrate pH 6 (Dako, Glostrup, Denmark) for 40 minutes at 95℃ and subsequently cooled for 20 minutes at room temperature in the same solution. The slide was washed in deionized water for 5 minutes and digested in protease solution with pepsin (0.5 mg/mL) (Sigma Aldrich, St Louis, MO) in 0.01 M HCl at 37 C for 20 minutes. The slide was then placed into deionized water for 5 minutes, dehydrated in a series of ethanol solutions (70%, 85%, 96% for 2 min each), and air-dried. Probes for aneuploidy detection of chromosomes 7, 17, and Y (Vysis/Abbott Molecular, IL) (Table 3) were mixed with water and CEP Hybridization buffer (Vysis) in a 1:2:7 ratio. An appropriate amount of probe mix and factory premixed XY probe was applied to each specimen, which was then covered with a glass coverslip and sealed with rubber cement. The slide was incubated in the ThermoBrite instrument (StatSpin/Iris Sample Processing, Westwood, MA) with codenaturation parameters of 85 C for 8 minutes and hybridization parameters of 37 C

for 16 hours. The rubber cemented coverslip was then removed, and the slide was placed in posthybridization wash solution (2 SSC/0.3% NP-40) at 721C for 2 minutes. The slide was air-dried in the dark, counterstained with 4, 6-diamidino-2-phenylindole (DAPI) (Vysis), coverslipped, and examined immediately.

Table 3. FISH Probes for detection of aneuploidy of chromosomes 7, 17, and Y

Chromosome	**Probe**
7	CEP 7 (D7Z1)/7p11.1-q11.1 Alpha Satellite DNA
17	CEP 17 (D17Z1)/17p11.1-q11.1 Alpha Satellite DNA
Y	CEP X (DXZ1) SpectrumGreen/CEP Y (DYZ3)//Yp11.1-q11.1 Alpha Satellite DNA/Xp11.1-q11.1 Alpha Satellite DNA

FISH – fluorescence in situ hybridization

The sections were examined with an Olympus BX51 fluorescence microscope (Olympus Corporation, Tokyo, Japan) using a 100 objective with Triple Band Pass (DAPI/SpectrumGreen/SpectrumOrange) and Single Band Pass (SpectrumGreen/ SpectrumOrange) filter sets.

4.7 *VHL* gene analysis

Mutation analysis of exons 1, 2, and 3 of the *VHL* gene was performed using polymerase chain reaction (PCR) and direct sequencing. PCR was carried out using the primers shown in Table 4. The reaction conditions were as follows: 12.5 mL of HotStar Taq PCR Master Mix (Qiagen), 10 pmoL of each primer, 100 ng of template DNA, and distilled water up to 25 mL. The amplification program consisted of denaturation at 95℃ for 15 minutes and then 40 cycles of denaturation at 95℃ for 1 minute, annealing at 55℃ for 1 minute, and extension at 72℃ for 1.5 minutes for all amplicons. The program was

finished by 72°C incubation for 7 minutes. The PCR products were checked on 2% agarose gel electrophoresis. Successfully amplified PCR products were purified with magnetic particles Agencourt AMPure (Agencourt Bioscience Corporation, A Beckman Coulter Company, Beverly, MA), both sides sequenced using Big Dye Terminator Sequencing Kit (Applied Biosystems, Foster City, CA) and purified with magnetic particles Agencourt CleanSEQ (Agencourt Bioscience Corporation) all according to the manufacturers' protocol. The samples were subsequently run on an automated sequencer ABI Prism 3130xl (Applied Biosystems) at a constant voltage of 13.2 kV for 20 minutes. All samples were analyzed in duplicates, and analysis of positive samples was repeated. For 3p loss of heterozygosity (LOH) analysis of neoplastic tissue DNA, 10 STR (short tandem repeats) markers: D3S666, D3S1270, D3S1300, D3S1581, D3S1597, D3S1600, D3S1603, D3S1768, D3S2338, and D3S3630 located on the short arm of chromosome 3 (3p) were chosen from the database (Gene Bank UniSTS). The primers are listed in Table 5. PCR conditions were the same as mentioned above. Successfully amplified PCR products were mixed with GeneScan 500 LIZ dye Size Standard (Applied Biosystems) and run on an automated genetic analyzer ABI Prism 3130xl (Applied Biosystems) at a constant voltage of 15 kV for 20 minutes.

A sample was considered LOH positive if the ratio of non-tumor DNA to tumor DNA was >1.5 or <0.66. All samples were analyzed in duplicates.

Table 4. PCR Primers used in mutation analysis of the *VHL* gene and designed in Primer3 software

Gene/Exon	Name	Primers (Sequence 5' → 3')
VHL/exon 1	VHL e1-1	CGCGAAGACTACGGAGGT
	VHL e1-2	GTCTTCTTCAGGGCCGTA
	VHL e1-3	GAGGCAGGCGTCGAAGAG
	VHL e1-4	GCGATTGCAGAAGATGACCT
	VHL e1-5	GCCGAGGAGGAGATGGAG
	VHL e1-6	CCCGTACCTCGGTAGCTGT
	VHL e1-7	CCGTATGGCTCAACTTCGAC
	VHL e1-8	GCTTCAGACCGTGCTATCGT
VHL/exon 2	VHL e2-1	ACCGGTGTGGCTCTTTAACA
	VHL e2-2	TCCTGTACTTACCACAACAACCTT
VHL/exon 3	VHL e3-1	GCAAAGCCTCTTGTTCGTTC
	VHL e3-2	ACATTTGGGTGGTCTTCCAG
	VHL e3-3	CAGGAGACTGGACATCGTCA
	VHL e3-4C	CCATCAAAAGCTGAGATGAAAC

PCR – Polymerase chain reaction

Table 5. PCR Primers used in LOH analysis of chromosome 3p

Marker	Name	Primers (Sequence 5' → 3')
D3S666	D3S666-SK#15	CAAGGCATTAAAGTGGCCACGC
	D3S666-SK#16	GTTTGAACCAGTTTCCTACTGAG
D3S1270	D3S1270-F	TGGAACTGTATCAAAGGCTC
	D3S1270-R	TTGCATTAGNATTCTCCAGA
D3S1300	D3S1300SF	AGCTCACATTCTAGTCAGCCT
	D3S1300A	GCCAATTCCCCAGATG
D3S1581	D3S1581-F	CAGAACTGCCAAACCA
	D3S1581-R	GGGTAACAGGAGCGAG
D3S1597	D3S1597-F	AGTACAAATACACACAAATGTCTC
	D3S1597-R	GCAAATCGTTCATTGCT
D3S1600	D3S1600-F	ATCACCATCATCTGCCTGTC
	D3S1600-R	TGCTTGCCTTGGGATTTA
D3S1603	D3S1603-F	CCCTAACTCCACTTGAAAGC
	D3S1603-R	TCAGCGAACAGCAACAAAT
D3S1768	D3S1768SF	GGTTGCTGCCAAAGATTAGA
	D3S1768A	CACTGTGATTTGCTGTTGGA

D3S2338	D3S2338-F	GAAGCCAGCAGTTTCTC
	D3S2338-R	CTGTATTGTTTTCCAGGATAAG
D3S3630	D3S3630-F	AAGGGATAAGCTGCAAATCA
	D3S3630-R	ACCAAATACAATTCATGAGACCTGA
	LOH – Loss of heterozygosity	

4.8 *FH* (Fumarate hydratase) gene mutation analysis

Three cases occurring in young patients (29, 31, 44 y) were further analyzed. DNA from FFPE tissue was extracted using a QIAsymphony DNA Mini Kit (Qiagen) on the automated extraction system (QIAsymphonySP, Qiagen) according to the manufacturer's supplementary protocol for FFPE samples (Purification of genomic DNA from FFPE tissue using the QIAamp DNA FFPE Tissue Kit and Deparaffinization Solution). The mutation of the whole coding sequence of the *FH* gene was performed using PCR and direct sequencing. PCR was carried out using the primers shown in Table 6. The reaction conditions were as follows: 12.5 mL of HotStar Taq PCR Master Mix (Qiagen), 10pmoL of each primer (Table 4), 100 ng of template DNA, and distilled water up to 25 mL. The amplification program consisted of denaturation at 95℃ for 15 minutes and then 40 cycles of denaturation at 95℃ for 1 minute, annealing at 60℃ for 1 minute, and extension at 72℃ for 1.5 minutes for all amplicons. The program was finished with 72℃ incubation for 7 minutes. The PCR products were checked on 2% agarose gel electrophoresis. Successfully amplified PCR products were purified with the magnetic particles Agencourt AMPure (Agencourt Bioscience Corporation, A Beckman Coulter Company), both sides sequenced using the Big Dye Terminator Sequencing Kit (Applied Biosystems) and purified with the magnetic particles Agencourt CleanSEQ (Agencourt) all according to the manufacturers' protocol. Subsequently, the sequencing products were

run on an automated sequencer ABI Prism 3130xl (Applied Biosystems) at a constant voltage of 13.2 kV for 20 minutes.

Table 6. PCR Primers used in *FH* gene mutation analysis

Primer name	Sequence 5' → 3'	Product size
FH-e1-F	GCGGAACGGTTTCTGACA	263
FH-e1-R	CAGGAGGGCTGAAGGTCACT	
FH-e2-F	GATGCGATTACTTTTGATCCTG	235
FH-e2-R	CCAAAATAGCCAACATTTCCA	
FH-e3-F	GCCAAAATAATAAACTTCCATGC	230
FH-e3-R	AGTATGGCATGGGTCTGAGG	
FH-e4-F	GGCATAATCAGCATTATTATTTCCTT	262
FH-e4-R	AAAAACAGCAAAGCTCACATACTG	
FH-e5a-F	TTTGTTTTTGTTGCCTCTGATTT	169
FH-e5a-R	GGATTTTGCATCAAGAGCATC	
FH-e5b-F	CTTTTCCCACAGCAATGCAC	218
FH-e5b-R	CATTTGTACCAAGCTCTAAATTGAA	
FH-e6a-F	CTTTGCTCATCATAAGATTTGAAGT	262
FH-e6a-R	CAACAGCAGTGCCTCCAG	
FH-e6b-F	TCAGGAATTTAGTGGTTATGTTCAA	224
FH-e6b-R	CAGACCACGTATAATGAGAAATGAA	
FH-e7a-F	TTGCTAATGGTAGAAAAATGTTTAGTT	200
FH-e7a-R	CCCAAAAATCGAATATCATTTGC	
FH-e7b-F	CTCATGACGCTCTGGTTGAG	197
FH-e7b-R	CAAGTTTTAGCTCCAACATTTACTAGC	
FH-e8-F	TTTCTTTATTCTCCTGATTATTTGCAT	249
FH-e8-R	CCAAGATAATAAGCCTTTGGTCA	
FH-e9-F	CTCTCTCTCTCTCTCTCTCTCACTCAC	244
FH-e9-R	TGGTTTAGCTTTTTAATTTTGCATT	
FH-e10-F	AACCCATATGTCGTCTTTTTATTTTT	245
FH-e10-R	TTTTTAAGAAATGGGAGTCTGTTTTT	

PCR – Polymerase chain reaction

4.9 Analysis of *VHL* promoter methylation

Detection of the *VHL* promoter methylation was carried out via methylation specific PCR as described elsewhere (67). Briefly, 100 ng of DNA or 2 μL of converted DNA was added to reaction consisted of 12.5 μL of HotStar Taq PCR Master Mix

(Qiagen), 10 pmol of forward and reverse primer and distilled water up to 25 μL. The amplification program comprised denaturation at 95°C for 14 minutes and then 40 cycles of denaturation at 95°C for 1 minute, annealing at 60°C for 1 minute, and extension at 72°C for 1 minute. The program was finished by incubation at 72°C for 7 minutes. The PCR products were checked on 2% agarose gel electrophoresis. A patient with known *VHL* mutation and fully methylated HeLa cell DNA were used as a positive control for *VHL* mutation analysis and promoter methylation analysis, respectively. As a negative control, randomly selected healthy donor blood was used.

4.10 Statistical analysis

The data were analyzed using SPSS version 19 (Chicago, IL, USA). Chi-square test was used to analyze the differences in morphologic criteria and immunohistochemical staining pattern and intensity. Fisher's exact test was used for dichotomous variables, and student t-test was used to compare mean Ki-67 percentages. Kaplan Meier Survival Analysis was used to analyze the overall survival across the tumor types. Cox-Mantel log-rank test was used to calculate the p-value for differences between the groups. A *p*-value of less than 0.05 was considered significant.

5 RESULTS

5.1 Cystic Renal Oncocytoma

5.1.1 Clinico-pathological characteristics

We evaluated 24 cases of the predominantly cystic variant of the RO and compared their clinicopathological properties with 30 conventional solid variants of this tumor to examine whether the two variants differ otherwise, except for their predominant architecture. The results are summarized in Table 7 and Table 8.

The patients' mean age was 68.7 years (range 51-85) in the cystic RO variant group and 60.3 years (range 24-85) in the conventional RO group. There were 17 (70%) male and 7 (30%) female patients in the cystic RO group (M:F ratio 2.43) and 21 (62%) males and 9 (28%) females in the conventional RO group (M:F ratio 1.63). The average size of the tumors was 25.6 mm (range 10-47 mm) in the cystic RO group and 32.1 mm (range 10-100 mm) in conventional RO.

The average follow-up duration was 33.6 months (range 12-108) in cystic RO and 68.6 months (range 2-128) in conventional RO. The status of the patients' follow-up is presented in Table 7.

Histological analysis revealed differences between the CRO and RO in architecture, frequencies of hemorrhage, and the amount and type of stroma. The morphological characteristics are summarized in Table 8 and Figure 3.

Table 7. Clinical properties of cystic renal oncocytoma (cRO) and conventional renal oncocytoma (RO)

	cRO	**RO**	***p*-value**
Number of cases (n)	24	30	
Age (years) (range)	68.7 (51-85)	61.6 (24-85)	$p>0.05$
Sex			
M	17	21	
F	7	9	
M:F ratio	2.43	1.63	
Size (mm) (range)	25.6 (10-47)	32.1 (10-100)	$p>0.05$
Follow up (months) (range)	33.6 (12-108)	68.6 (2-128)	
AW (n)	10	21	
DOD	0	3	
DD	0	0	
LFU	14	6	

M – male, F – female, AW – Alive and well, DOD – died of other diseases, DD – died of disease, LFU – lost for follow-up. $p<0.05$ was considered significant.

5.1.2 Immunohistochemical properties

The immunohistochemical properties of the CRO are summarized in Table 9. cRO shows an immunohistochemical profile similar to the solid RO variant with diffuse positivity for CAM5.2, CD117, OSCAR, MIA, and scattered staining pattern for CK7 in most of the cases. CRO is mostly negative for CAIX and CD10 staining.

Table 8. Morphological characteristics of the cystic renal oncocytoma (cRO) and conventional renal oncocytoma (RO)

	cRO (n=24)	**RO (n=30)**	***p* value**
Architecture			
Tubules/cysts (mean volume %)	76.8	4.0	
Solid (mean volume %)	10.7	86.0	***p*<0.01**
Islands/nests (mean volume %)	12.0	10.8	
Papillary/micropapillary budding in cysts [n(%)]			
Yes	3 (12)	1 (2)	
No	21 (88)	29 (98)	
Lining of the cysts [n (%)]			
Single cell layer	20 (83.3)	1 (2.0)	
Pseudopapillary	2 (8.3)	0 (0.0)	
Multilayered	2 (8.3)	0 (0.0)	
Hemorrhage [n (%)]			
None	3 (12.5)	27 (90.0)	
Tubules/cysts	17 (70.8)	1 (2.0)	
Tubules/cysts and stroma	4 (16.7)	0 (0.0)	
Stroma	0 (0.0)	2 (8.0)	
Type of stroma [n (%)]			
Loose	19 (79.2)	2 (6.0)	
Loose and fibrotic	3 (12.5)	24 (80.0)	***p*<0.01**
Fibrotic	2 (8.3)	4 (14.0)	
Amount of stroma			
Scant	12 (50.0)	25 (82.0)	
Moderate	9 (37.5)	4 (16.0)	
Abundant	3 (3.0)	1 (2.0)	
Cytology [n (%)]			
Dominant oncocytic	24 (100)	29 (98.0)	
Focal oncocytic	0 (0.0)	1 (2.0)	
Nucleolar grade [n (%)]			
1	13 (54.2)	17 (58.0)	
2	10 (41.7)	11 (36.0)	
3	1 (4.2)	2 (6.0)	
4	0 (0.0)	0 (0.0)	
Mitotic figures [n (%)]			
Yes	0 (0.0)	0 (0.0)	
No	24 (100.0)	30 (100.0)	
Necrosis [n (%)]			
Yes	0 (0.0)	0 (0.0)	
No	24 (100.0)	30 (100.0)	

cRO – cystic renal oncocytoma, RO – renal oncocytoma. $p<0.05$ was considered significant and was shown where appropriate.

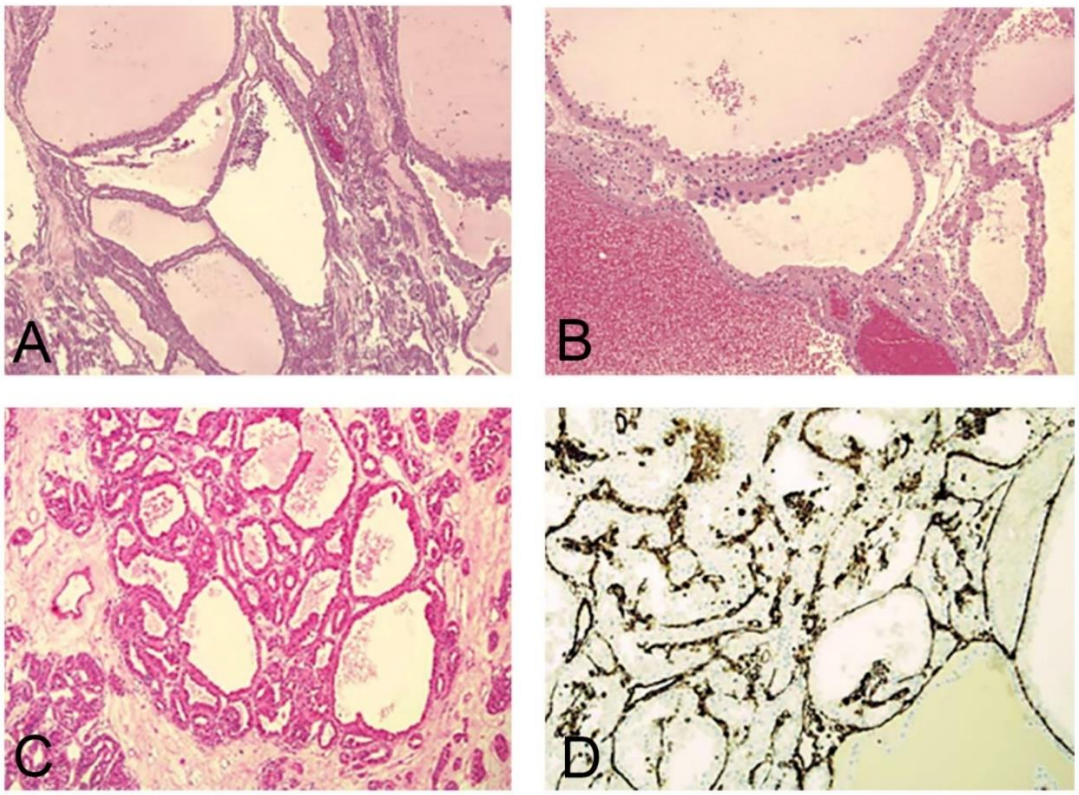

Figure 3. (A) The morphology of the cystic renal oncocytoma (CRO) shows predominantly cystic architecture. (B) Cells lining cysts are relatively uniform, voluminous, cuboidal, arranged in a single row. (C) Areas of prominent stroma with isolated islands of oncocytic cells are typical for cRO. (D) Immunoreactivity for vimentin shows negative staining in the cRO cells.

Table 9. Immunohistochemical properties of the cRO and RO

Antibody/tumor	cRO (n=24) (%)	RO (n=30) (%)	*p*-value
AMACR	33	27	
CK7	0 sc	0 sc	
CAIX	5 f	0	
CD117	100	100	
PAX8	80	64	
Vimentin	5	9	
Cathepsin K	2	3	
CD10	4 f	9 w	
CAM5.2	100	91	
AE1/AE3	80	64	
OSCAR	100	100	
TFE3	0	0	
EMA	82	64	
MIA	96	100	
Ki67	4.9	3	

sc – scattered cells positivity in less than 5% cells; w – weak staining; f – focal staining; cRO – cystic renal oncocytoma, RO – renal oncocytoma. $p<0.05$ was considered significant and was shown where appropriate.

5.2 Tubulocystic RCC

5.2.1 Clinico-pathological characteristics

Tubulocystic RCC was a recently established, distinct tumor entity. It does not have its solid counterpart. We thoroughly analyzed and characterized 15 institutional and consultation cases of this newly established tumor by the WHO.

The mean age of the patients was 59.8 years (range, 28-78 years). There were 10 (66.6%) male and 5 (33.4%) female patients in this group (M:F ratio 2.0). The average size of the tumors was 44.5 mm (range, 10-90 mm). Eleven cases were stage pT1, three were pT2, and one case was stage pT3.

Clinically and grossly, tumors presented as solitary, well-circumscribed masses. They were mostly composed of closely packed well-formed tubular and cystic structures separated by thin fibrous septa. This architecture was present with an average of 86.7% tumor volume. The small papillary budding was present in more than half of the cases. Stroma was scant and fibrotic in most of the cases. Mitoses and necrosis were occasionally found (Figure 4 and Table 10). The epithelial cells lining the cysts were eosinophilic with cylindrical, cuboidal, flattened, or hobnail appearance. The lining cells contained prominent nucleoli, mostly equivalent to ISUP nucleolar grade 3.

Six cases had pure TCRCC morphology. Another five cases contained distinctive and separate PRCC-like areas (mostly PRCC type 1 like) in the association with TCRCC (Figure 4 C-D). Three cases showed TCRCC morphology with PRCC-like areas, high-grade renal cell carcinoma (HGRCC NOS) (Figure 5), or CCPRCC/RAT-like features. The TCRCC with CCPRCC/RAT-like areas presented at an advanced stage and had a fatal outcome due to metastatic disease within one year of surgery. The last case had classic TCRCC architecture and cytological appearance but large prominent nuclei and conspicuous red nucleoli. It was later reclassified using molecular genetic analysis as hereditary leiomyomatosis-associated RCC (HLRCC) (Figure 4). Tumors with intermixed TCRCC and PRCC architecture were excluded from the study (Figure 6).

The average follow-up duration was 47.5 months (range, 12-108 months). Ten patients with pure TCRCC and TCRCC with PRCC-like areas were alive and well. One patient with a tumor reclassified as HLRCC was alive with advanced metastatic disease. Four patients later reclassified as non-TCRCC based on heterologous component and molecular findings had an adverse outcome on follow-up and died. Three of the deceased

patients were younger than 45 years (2 males, 29 and 44 years old, and 1 female, 31 years old).

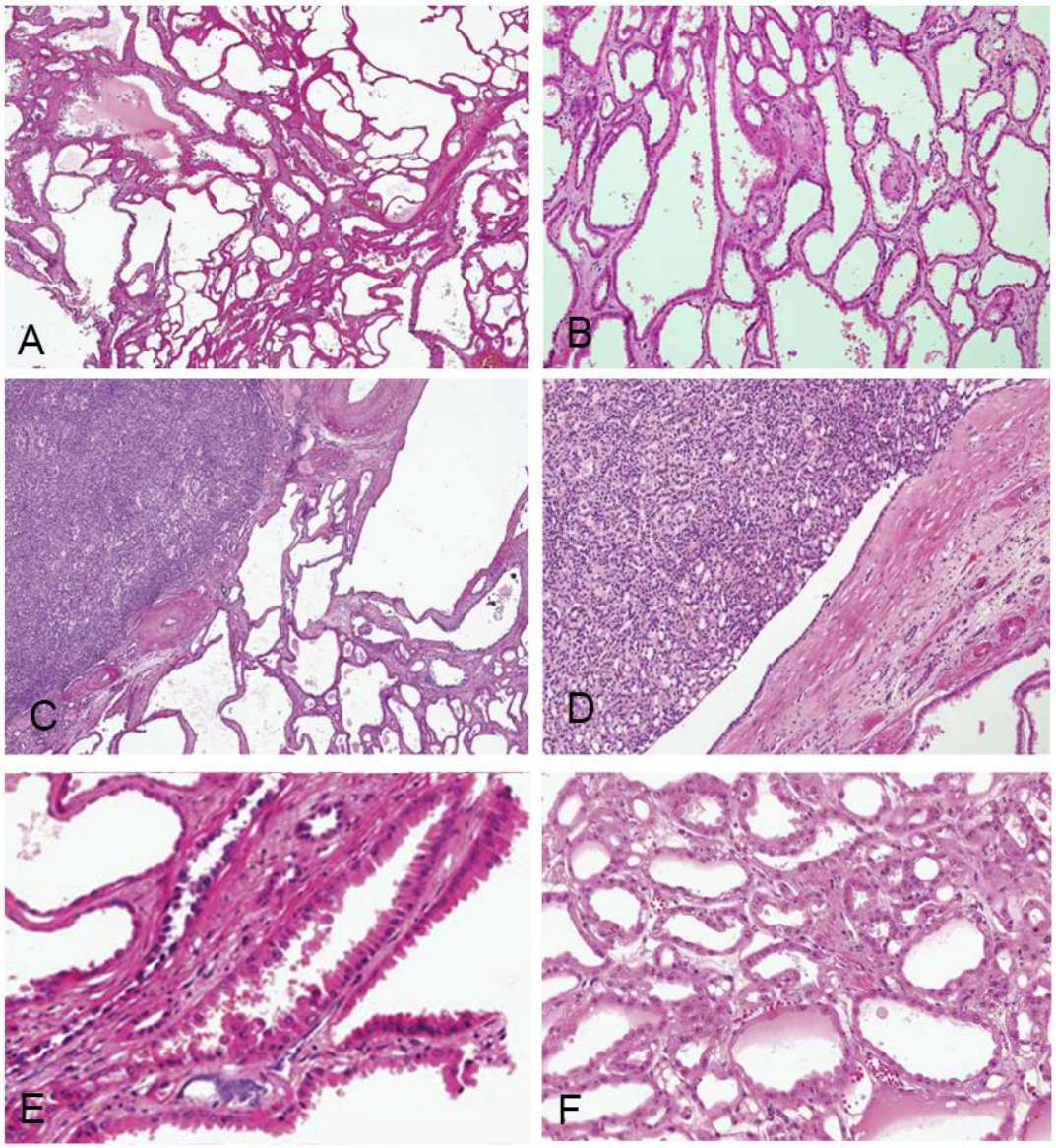

Figure 4. Morphological properties of Tubulocystic renal cell carcinoma (TCRCC). (A, B) Low power magnification shows typical tubulocystic renal cell carcinoma architecture presented by closely packed well-formed tubules and cysts separated by thin fibrous septa. (C, D) Papillary renal cell carcinoma-like areas were frequently associated with TCRCC. (E) Cysts were lined with eosinophilic with cylindrical, cuboidal, flattened, or hobnail cells appearance. (F) One case with typical TCRCC morphology was later reclassified as hereditary leiomyomatosis-associated renal cell carcinoma using molecular genetic testing.

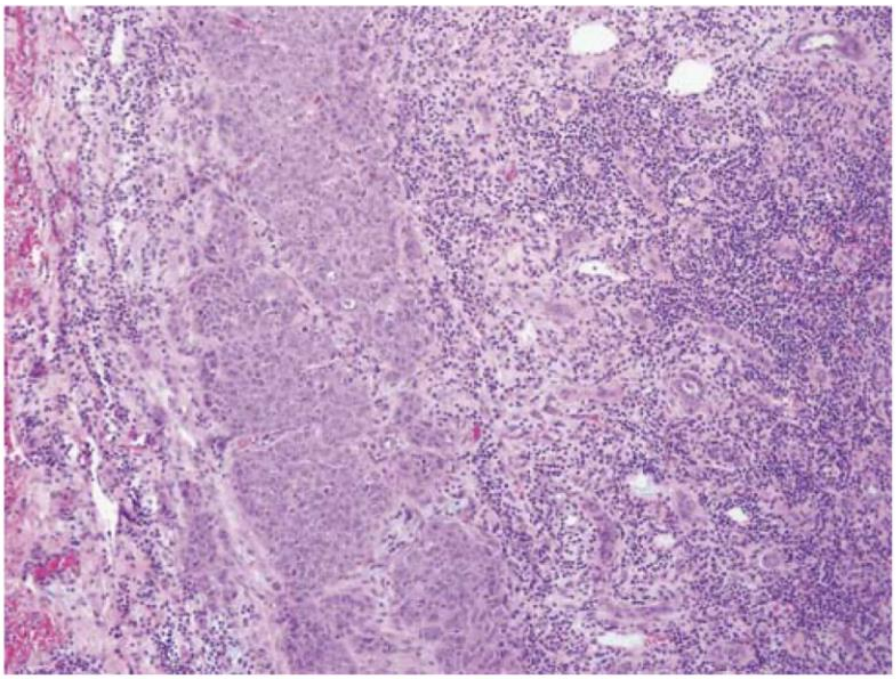

Figure 5. Two cases of TCRCC contained foci of high-grade renal cell carcinoma (NOS).

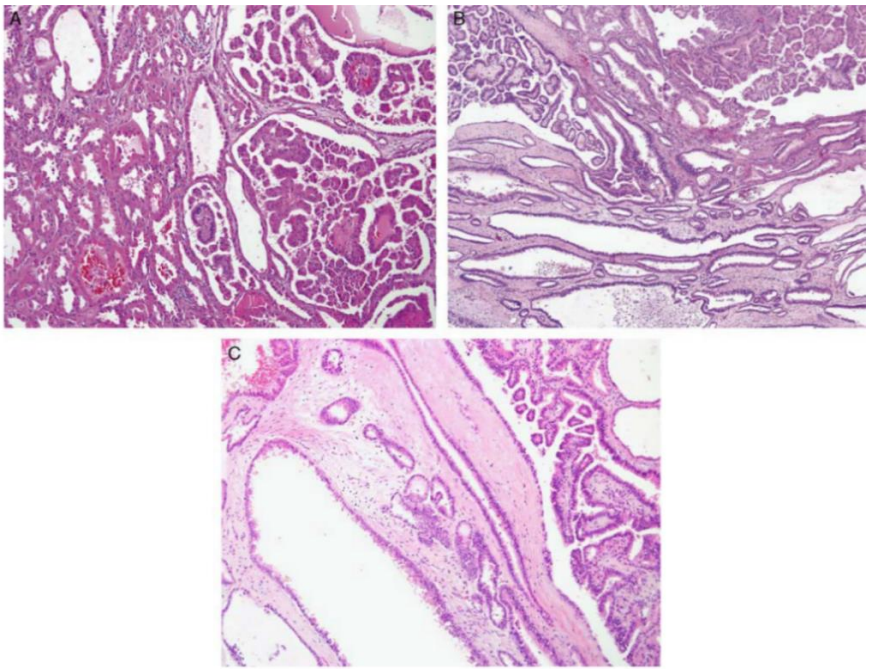

Figure 6. Intermixed TCRCC and PRCC architecture. These tumors were excluded from the study.

Table 10. Morphological features of TCRCC

	TCRCC (n=15)
Architecture	
Tubules/cysts (mean volume %)	86.7
Solid (mean volume %)	2.0
Islands/nests (mean volume %)	1.8
Papillary/micropapillary budding in the cysts [n(%)]	
Yes	9 (60.0)
No	6 (40.0)
Lining of the cysts [n (%)]	
Single cell layer	6 (40.0)
Pseudopapillary	6 (40.0)
Multilayered	3 (20.0)
Hemorrhage [n (%)]	
None	5 (33.3)
Tubules/cysts	3 (20.0)
Tubules/cysts and stroma	3 (20.0)
Stroma	4 (26.7)
Type of stroma [n (%)]	
Loose	1 (6.7)
Loose and fibrotic	2 (13.3)
Fibrotic	12 (80.0)
Amount of stroma	
Scant	13 (86.7)
Moderate	2 (13.3)
Abundant	1 (6.7)
Cytology [n (%)]	
Dominant oncocytic	9 (60.0)
Focal oncocytic	6 (40.0)
Nucleolar grade [n (%)]	
1	1 (6.7)
2	5 (33.3)
3	9 (60.0)
4	0 (0.0)
Mitotic figures [n (%)]	
Yes	4 (26.6)
No	11 (73.3)
Necrosis [n (%)]	
Yes	4 (26.7)
No	11 (73.3)

TCRCC – tubulocystic renal cell carcinoma

5.2.2 Immunohistochemical properties

Immunohistochemically, TCRCC showed diffuse staining for CAM5.2, MIA, OSCAR, and variable positivity for EMA and CA-IX. CD117 was negative in 93.3% of cases, and vimentin and AMACR were mostly positive, with a Ki-67 proliferative index of 17.93. Immunohistochemical findings are summarized in Table 11.

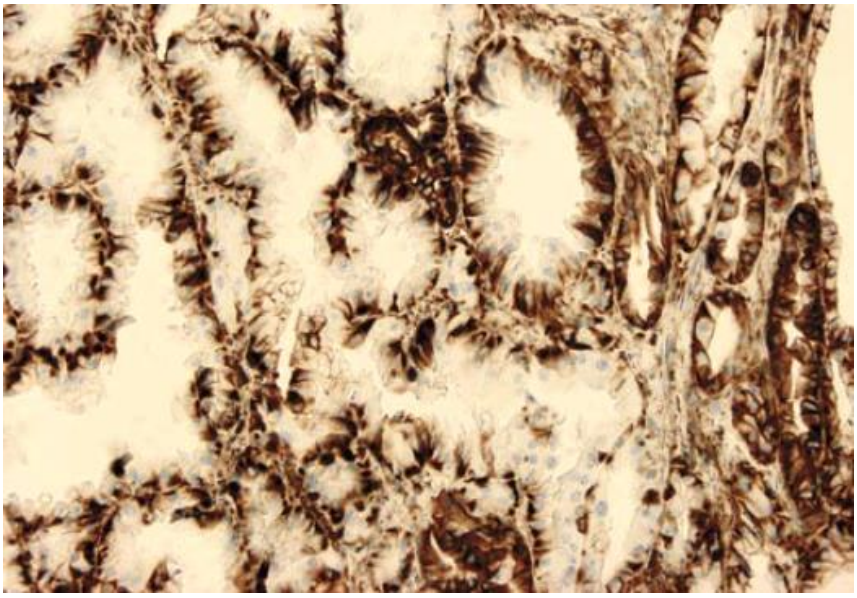

Figure 7. Vimentin staining in TCRCC shows diffuse positivity in 80% of the cases.

Table 11. Immunohistochemical properties of the TCRCC

antibody	**TCRCC (n=15) (%)**
AMACR	87
CK7	70 p
CAIX	43 p
CD117	6
PAX8	93
Vimentin	93
Cathepsin K	0
CD10	70
CAM5.2	100
AE1/AE3	100
OSCAR	100
TFE3	0
EMA	77
MIA	100
Ki67	17.9

TCRCC – tubulocystic renal cell carcinoma; p – patchy staining pattern

5.2.3 Molecular genetic properties

We used FISH, PCR, and direct sequencing to analyze the most common genetic abnormalities reported in renal carcinomas to elucidate the molecular profile and the position of this renal carcinoma subtype within the renal carcinoma family. Structural and numerical chromosomal abnormalities of chromosomes 7, 17, Y were analyzed with FISH, while PCR and direct sequencing were used to analyze the *VHL* and *FH* gene mutations.

Chromosomes 7 and 17 were successfully analyzed in 13 and 14 cases, respectively, in the areas showing TCRCC morphology. Chromosome 7 was disomic and polysomic in 9 and 4 cases, respectively. Chromosome 17 was disomic and polysomic in

6 and 8 cases, respectively. Chromosome Y was normal in 3 cases and polysomic in 1 case, while another showed loss of chromosome y. In summary, the most frequent aberrancies were disomic chromosome 7 and polysomic chromosome 17. In 2 cases, chromosome 7 disomy, a gain of 17, and normal Y was found. The case has later proven to be HLRCC had chromosome 7 and 17 polysomy with a gain of Y in TC-RCC-like areas, and chromosome 7 disomy, a gain of 17, and normal Y in PRCC-like areas. One of the 2 cases with foci of HGRCC was not analyzable due to the insufficient number of tumor cells. The HGRCC area in the second tumor showed disomic chromosome 7, polysomic chromosome 17, and normal Y. This tumor also contained a PRCC focus that showed the same status of chromosomes 7 and Y, with a gain of chromosome 17. The TCRCC component in this tumor was disomic for chromosome 7 and polysomic for chromosome 17.

In the single case with a CCPRCC/RAT-like pattern, both components (CCPRCC/RAT and TCRCC) showed gains of chromosomes 7 and 17. In addition, mutation of the VHL gene and LOH 3p were found in the CCPRCC/RAT-like area.

Three cases with aggressive forms of TC-RCC (patients being younger than 45 at the time of diagnosis) were analyzed for mutations of the FH gene. One was not analyzable due to the low quality of DNA, one was negative for mutations, and one showed a deletion of exon 7 of the FH gene: c.911_917delCTTTTGT, p.(Phe305Leufs*22).

Table 12. Histologic patterns and chromosome 7, 17, and Y status in TCRCC cohort

Case #	Histologic pattern (%)	Chromosome 7	Chromosome 17	Chromosome Y
1	TCRCC (100)	polysomy	disomy	normal (XY)
2	TCRCC (100)	NA	polysomy	NA
3	TCRCC (100)	disomy	polysomy	NP
4	TCRCC (100)	disomy	polysomy	NP
5	TCRCC (100)	disomy	disomy	NP
6	TCRCC (100)	disomy	disomy	loss (X0)
7	TCRCC (95)	polysomy	polysomy	polysomy (XYY)
	PRCC (5)	disomy	polysomy	normal (XY)
8	TCRCC (60)	disomy	polysomy	normal (XY)
	PRCC (40)	polysomy	polysomy	X polysomy (XXY)
9	TCRCC (90)	disomy	disomy	NA
	PRCC (10)	NA	NA	NA
10	TCRCC (95)	disomy	polysomy	NA
	PRCC (5)	NA	NA	NA
11	TCRCC (99)	polysomy	disomy	normal (XY)
	PRCC (1)	NA	NA	NA
12	TCRCC (99)	disomy	disomy	NP
	PRCC (1)	NA	NA	NP
13	TCRCC (70)	disomy	polysomy	NA
	PRCC (25)	disomy	polysomy	normal (XY)
	HGRCC (5)	disomy	polysomy	normal (XY)
14	TCRCC (95)	NA	NA	NA
	HGRCC (5)	NA	NA	NA
15	TCRCC (50)	polysomy	polysomy	NP
	RAT (50)	polysomy	polysomy	NP

TCRCC – tubulocystic renal cell carcinoma; PRCC – papillary renal cell carcinoma; HGRCC – high-grade renal cell carcinoma; RAT – renal angiomyomatous tumor; NA – not analyzable; NP – not performed

5.3 Cystic Papillary RCC

5.3.1 Clinico-pathological characteristics

Papillary RCC is the second most frequent kidney cancer with well-established and described histologic type 1 and type 2 variants confirmed by molecular profiling. Type 2 is further molecularly subdivided (68). Rarely, this tumor may present with abundant necrosis, cystic and pseudocystic architecture. We aimed to characterize the

cystic and necrotic variant of PRCC type 1 (cPRCC) and compare the data with the conventional papillary variant.

We retrieved 10 cases from our institutional archives and external consultation cases and compared them with 27 cases of the conventional variant of this tumor. The patients' mean age was 62.6 years (range, 32-85 years) in the cPRCC group and 54.4 years (range, 20-84 years) in the conventional PRCC variant. There were 8 (80%) male and 2 (20%) female patients in the cPRCC group (M:F ratio 4.0), and 15 (56%) male and 12 (44%) female in the conventional PRCC group (ratio M:F 1.27). The average size of the tumors was 94 mm (range, 60-140 mm) in cPRCC and 35.3 mm in the conventional PRCC group ($p<0.05$). Two cases were in the pT1b stage, while the rest of the tumors were in the pT2 stage in cPRCC. In PRCC 17/27 cases were pT1a, 9/27 cases pT1b, and one case pT2a ($p<0.05$).

In the cPRCC group, the average follow-up duration was 48 months (range, 5–128 months). Seven patients were alive and well at the time of the study, while three patients died of conditions unrelated to PRCC progression (lung cancer and hepatic failure). In the conventional PRCC group, the average follow-up duration was 42.2 months (range 16-92). Similar to the cPRCC group, most of the patients (25/27) were alive and well at the study time, while only 2/27 died of conditions unrelated to kidney cancer.

Grossly, tumors were well-circumscribed, unilocular cystic mass, encapsulated by thick fibrous tissue, with the inner surface lined by a thin brownish friable tissue cystic space filled with hemorrhagic and necrotic material (Figure 8).

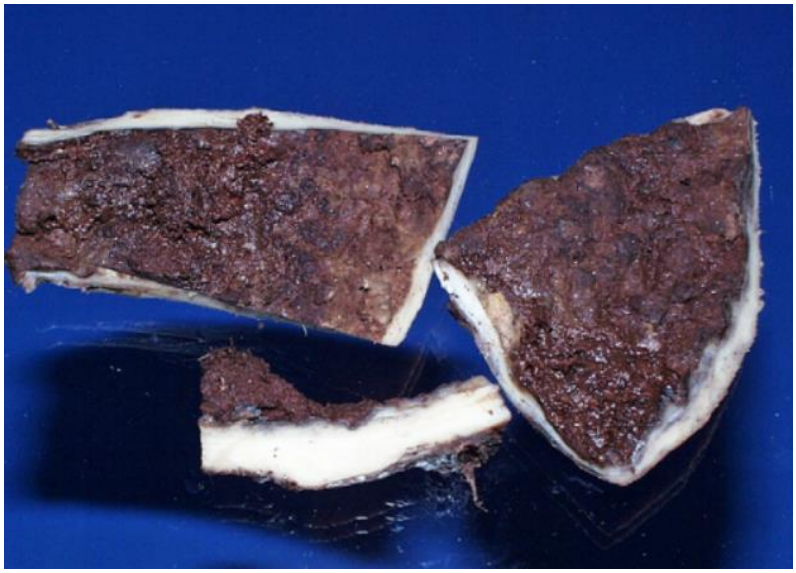

Figure 8. Cystic and necrotic Papillary Renal Cell Carcinoma. The tumor was surrounded by think whiteish fibrous tissue, and the cystic space was filled with hemorrhagic and necrotic material.

Microscopically, most of the tumors showed basophilic appearance with low-grade nuclei, consistent with the PRCC type 1. In most cases, the central part of the tumor was largely necrotic, while peripheral parts contained viable neoplastic cells focally forming short papillae, micropapillae or tubulopapillary structures (Figure 9 A, D). The papillary structures were lined by a single layer of cuboidal or low columnar cells with scant cytoplasm and uniform nuclei (Figure 9 C).

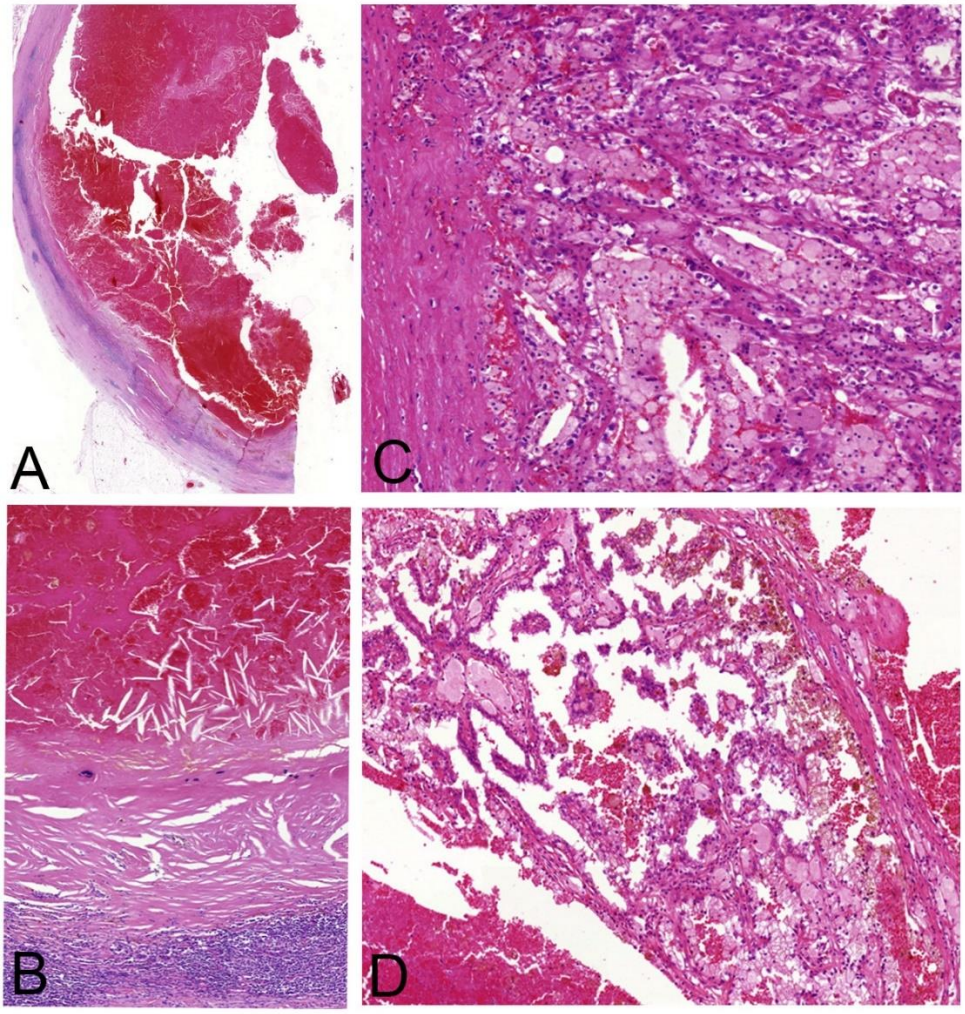

Figure 9. Microscopic appearance of the cystic papillary renal cell carcinoma (cPRCC). (A) A limited amount of the vital neoplastic tissue was present at the peripheral parts of the tumor, lining the thick fibrous-walled cyst. (B) Large central areas of the inner surface of the cyst were covered by necrotic material. (C-D) Viable neoplastic tissue formed tubulopapillary or short papillary structures mostly lined by single-layer cuboidal or low-columnar epithelial cells with scant cytoplasm and uniform nuclei.

5.3.2 Immunohistochemical properties

On immunohistochemical analysis of the cPRCC, 10/10 (100%) of tumors were diffusely positive for OSCAR, CAM5.2, vimentin, and AMACR (Table 13 and Figure 10). All the cases were also positive for CD117; however, the staining was weak. MIA was diffusely positive in 9/10 (90%) cases, and in one case, the positivity was focal. PAX8 was diffusely positive in 7/10 (70%) of cases, while in 3/10 (30%), the staining

was only focally positive. CAIX and TFE3 were negative in all the cases. Cathepsin K, and AE1-AE3 showed variable expression. The same antibodies showed similar staining percentages, patterns, and intensities across the conventional PRCC type 1 group, except the CD117, which was weekly positive in all cPRCC cases while mostly negative in conventional PRCC.

Table 13. Immunohistochemistry analysis of cPRCC and PRCC cohorts.

antibody/tumor	**cPRCC (n=10) (%)**	**PRCC (n=27) (%)**	***p*-value**
AMACR	100	92	
CK7	90	92	
CAIX	0	0	
CD117	100 w	14	***p*<0.01**
PAX8	100	92	
Vimentin	100	60	***p*<0.05**
Cathepsin K	20 w	7	
CD10	70	61	
CAM5.2	100	92	
AE1/AE3	100 p	92	
OSCAR	100	100	
TFE3	0	0	
EMA	90	84	
MIA	90	100	
Ki67	6	5	

w – weak staining intensity; p – patchy staining; cPRCC – cystic papillary renal cell carcinoma, PRCC – papillary renal cell carcinoma (conventional, type 1). $p<0.05$ was considered significant and was shown where appropriate.

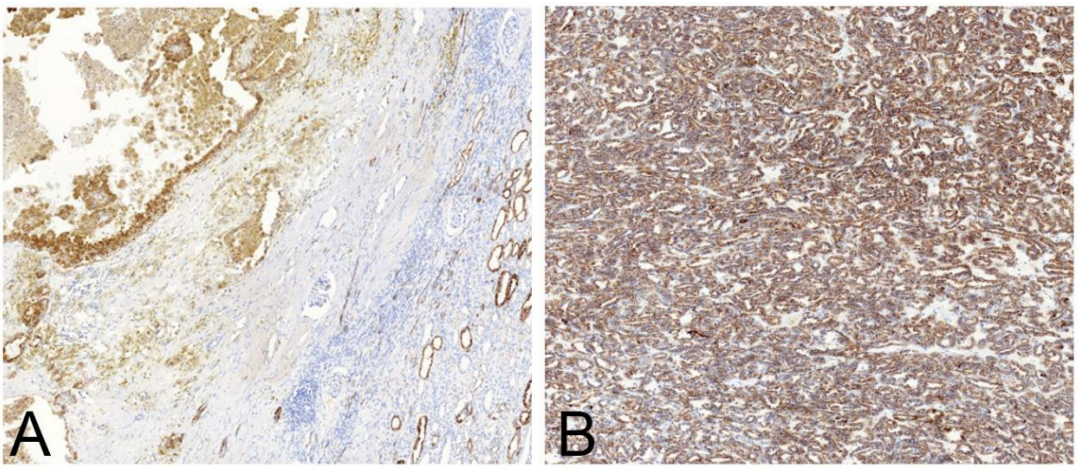

Figure 10. AMACR immunohistochemistry staining in (A) cPRCC and (B) PRCC type 1. The cells were uniformly positive in both tumor variants.

5.3.3 Molecular genetic properties

Next, we used aCGH and FISH to investigate the copy number variation in cystic PRCC. The most common finding was polysomic chromosome 7 and 17, found in 5/10 (50%) cases. In addition, one case showed a gain of chromosomes 7, 12, 13, 16, and 17 and loss of chromosome 21. Loss of chromosome Y was found in one case, with a gain of 9, 12, and 20. Two cases showed no chromosomal numerical aberrations (Figure 11 and Table 14).

VHL gene abnormalities, including mutations, hypermethylation of *VHL* promoter, and loss of heterozygosity of 3p locus, were not found in any cases (Table 14).

Table 14. Molecular genetic findings in cystic papillary renal cell carcinoma

Case #	sex	aCGH	Chr7	Chr17	ChrX/Y	LOH 3p	VHLmut	VHLmet
1	M	+9,+12,+20,-Y	D	D	-Y	Neg	Neg	Neg
2	F	+12,+13,+16,+17,-21	D	P	XX	Neg	Neg	Neg
3	M	No changes	NA	NA	NA	Neg	Neg	Neg
4	M	NP	D	P	-Y	NA	NA	Neg
5	F	NP	NP	NP	NP	NP	NP	NP
6	M	+7, +17	P	P	-Y	Neg	Neg	Neg
7	M	+(7pter-7q22.1),+17,-Y	P	P	-Y	NA	Neg	Neg
8	M	No changes	P	D	XY	Neg	Neg	Neg
9	M	+2,+3,+7,+12,+16,+17,+20,+21,+22	P	P	XY	Neg	Neg	Neg
10	M	NP	P	P	-Y	NA	Neg	Neg

aCGH - Array comparative genomic hybridization; Chr 7 – chromosome 7, Chr17 – chromosome 17; ChrX/Y – sex chromosome status; LOH – loss of heterozygosity; VHLmut – *VHL* gene mutation; VHLmet – *VHL* gene methylation; NA – not analyzable; NP – not performed; Neg – negative for mutation or methylation; D – disomy; P - polysomy

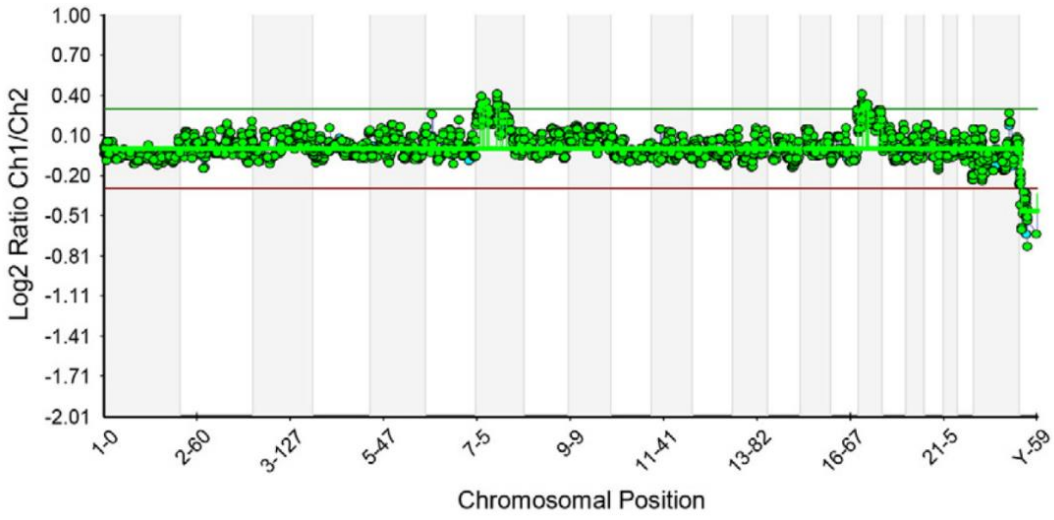

Figure 11. Array CGH profile of case 7 revealing gains on chromosomes 7 (7pter-7q22.1) and 17, and loss of chromosome Y.

5.4 Cystic Chromophobe RCC

5.4.1 Clinico-pathological characteristics

Chromophobe RCC is the third most common kidney cancer, with a frequency of about 5% of all renal tumors. We analyzed a rare cystic variant of this tumor and compared it with its common solid form.

We retrieved 10 cases of cystic ChRCC (cChRCC) from our institutional archives and external consultation cases and compared them with 20 cases of the conventional solid variant of this tumor. The patients' mean age was 68 years (range 50-89 years) in the cChRCC group and 61.4 years (range 17-83 years) in the conventional ChRCC variant. There were 6 (60%) male and 4 (40%) female patients in this cChRCC group (M:F ratio 1.5) and 11 (55%) male and 9 (45%) females in the conventional ChRCC group (ratio M:F 1.25). The average size of the tumors was 53.22 mm (range 12-200 mm) in the cChRCC, and 53-6 mm in the conventional ChRCC group ($p>0.05$). Six of ten cases (60%) were pT1a stage, 2/10 (20%) were pT1b, 1/10 (10%) was pT2 stage, while the staging was missing for one case for cChRCC. Eight of 20 cases were pT1a (40%), 6/20 (29%) cases were pT1b, 5/20 (25%) pT2, and 1/20 (3%) was pT3 in conventional ChRCC group.

In the cChRCC group, the average follow-up duration was 66 months (range 12–128). None of the patients died of kidney cancer. Six patients (60%) were alive and well at the time of the study; one died of an unrelated disease (10%), and three were lost for follow-up. In the ChRCC group, the average follow-up duration was 40.7 months (range 25-110). The majority of the patients (14/20, 70%) were alive and well at the time of the

study, 3/20 (15%) died of a condition unrelated to kidney cancer, and another 3/20 (15%) died of the disease.

Grossly, cChRCC were well-demarcated. Invasion into the blood vessels, renal sinus, pelvicalyceal system, or perirenal fat was not found. The tumor cut surface was brown or tan/yellow or gray.

The cells of most of the tumors were eosinophilic/oncocytic (6/10) or pale and leaf-like (3/10), while one case showed a mixed cell population. All the cases demonstrated typical morphological signs of chRCC, such as raisinoid nuclei and perinuclear halo. Binucleated cells were seen occasionally. According to the Paner grading system (grade 1 or 2), all the cases were low grade, without grade 3, or sarcomatoid differentiation.

Histologically, the tumors showed a prominent multicystic pattern with irregularly sized and shaped cysts and focal glandular cribriform pattern. Septa of the cysts were thin, lined mainly by a single layer of neoplastic cells. Occasionally larger aggregates of mostly eosinophilic/oncocytic cells were present within the septa. Deposits of dark brown pigment (lipofuscin and hemosiderin) were focally present in half of the cases. Dystrophic calcification was noted in four cases, while necrosis was not present (Figure 12 A-B). A smaller number of tumors (3/10) had a more solid appearance due to compressed elongated tubules resembling a solid architectural appearance. However, no proper solid areas were seen (Figure 12 E-F). The lumina of the compressed elongated tubules displayed a slit-like pattern (Figure 12 F).

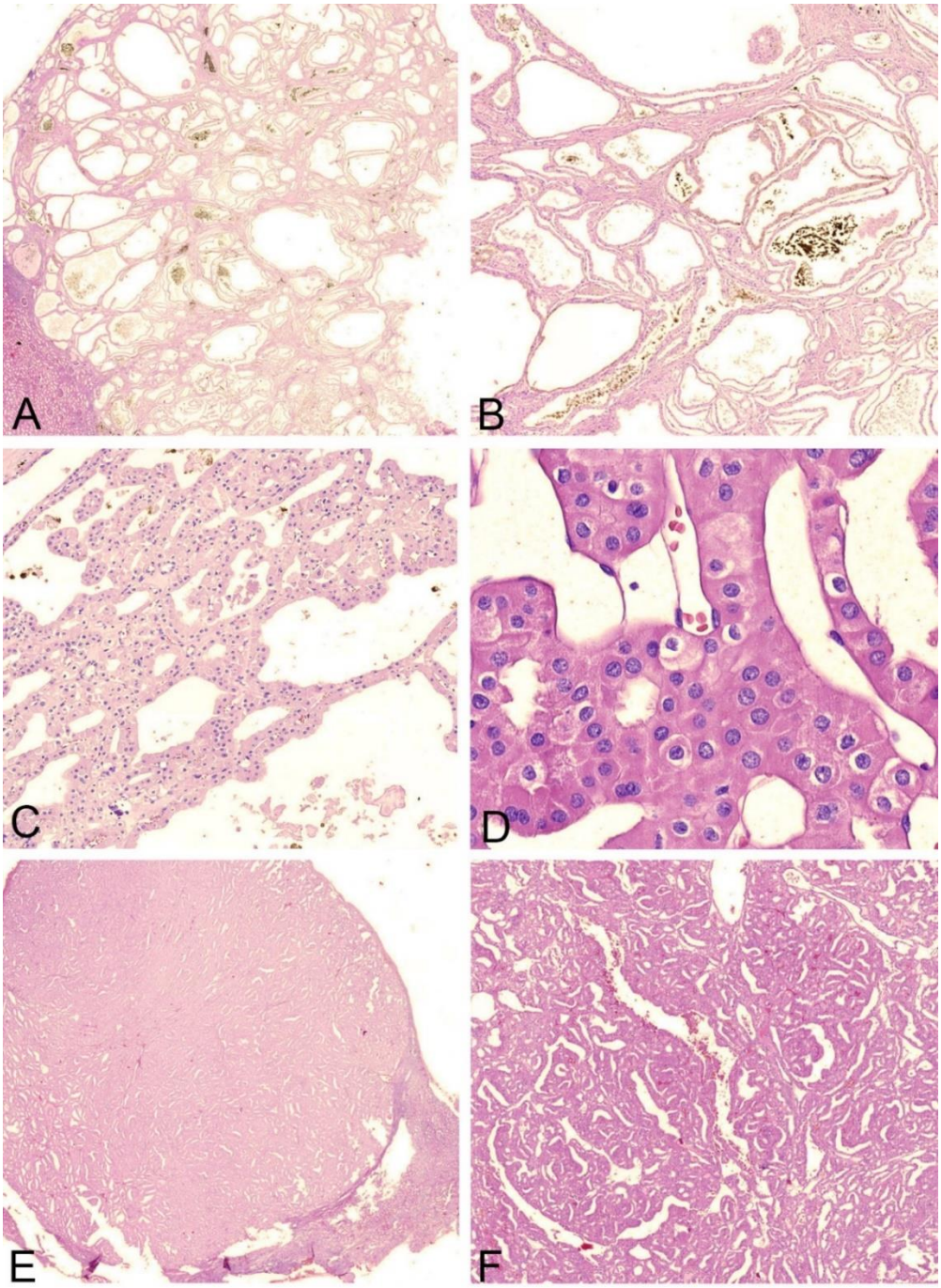

Figure 12. Morphology of the cystic chromophobe Renal cell carcinoma. (A) Multicystic architecture in a cystic variant of chromophobe renal cell carcinoma. (B) Dark brown lipochrome pigment was present within cystic spaces. (C, D) Tumors were composed of large eosinophilic or pale cells with raisinoid nuclei and perinuclear halo. (E, F) Some of the tumors showed compressed tubular and cystic spaces.

5.4.2 Immunohistochemical properties

Immunohistochemically, cChRCC were positive for CK7, OSCAR, CD117, EMA, antimitochondrial antigen, and PAX8. CK7 positivity was moderate to strong, with a somewhat patchy pattern in seven cases. Immunoreactivity for CD117 was diffuse but varied in intensity, ranging from weak (three cases) to strong (four cases). As indicated by nuclear Ki-67 staining, proliferation activity was very low (<1 %) in all cases. All the cases were negative for vimentin, AMACR, CAIX, TFE3, cathepsin K (Table 15 and Figure 13).

Table 15. Immunohistochemistry of the cystic chromophobe renal cell carcinoma

Antibody/tumor	**cChRCC (n=10) (%)**	**ChRCC (n=20) (%)**	***p*-value**
AMACR	0	12	
CK7	100 p	92	
CAIX	0	0	
CD117	100	100	
PAX8	100 w	90	
Vimentin	0	0	
Cathepsin K	0	0	
CD10	10	7	
CAM5.2	70	61	
AE1/AE3	100 p	92	
OSCAR	100	90	
TFE3	0	0	
EMA	100	84	
MIA	100	92	
Ki67	1	1	

w – weak staining intensity; p – patchy staining; cChRCC – cystic chromophobe renal cell carcinoma, ChRCC – chromophobe renal cell carcinoma (conventional). $p<0.05$ was considered significant and was shown where appropriate.

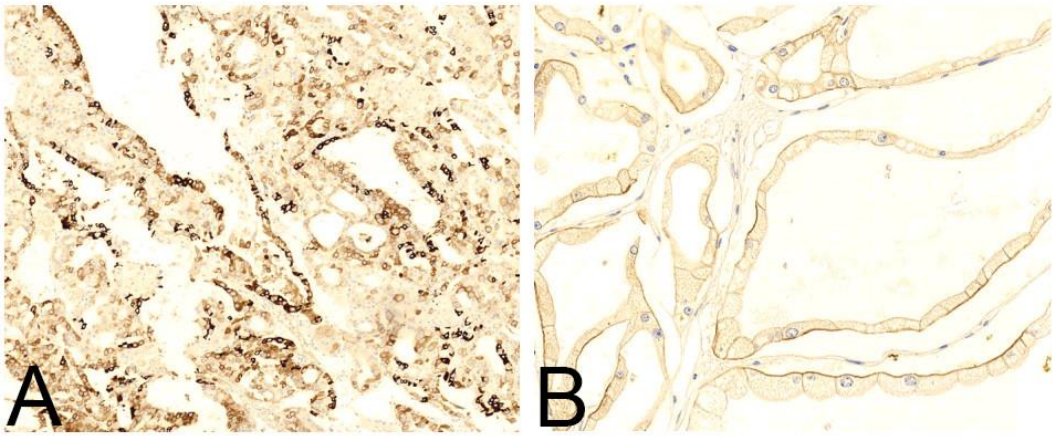

Figure 13. Immunohistochemical staining of cystic chromophobe carcinoma shows (A) consistently positive CK7 staining with a patchy pattern, and (B) CD117 staining.

5.4.3 Molecular genetic properties

We performed an aCGH analysis to analyze the ploidy status of the cChRCC. Multiple losses of chromosomes 1p, 2q, 6, 13, 17, 21, and X were found in two cases. Three cases showed no numerical chromosomal aberrations.

5.5 Immunohistochemical profiles of the cystic renal tumors

We pooled the data to compare the immunohistochemistry profiles of the different cystic renal tumor variants to get a better overview of the biomarkers involved in pathogenesis and evaluate their diagnostic usefulness. The data are summarized in Table 16.

PAX8 is expressed in all cystic renal tumor types and is considered a helpful marker for distinguishing metastatic renal neoplasia from other metastases. AMACR is positive in cPRCC and TCRCC, but is entirely or primarily negative in cRO and cChRCC.

CAIX is variable positive only in TCRCC, while negative in other cohorts. CK7 was positive in cChRCC, negative in cRO, and variably positive in cPRCC and TCRCC. Pankeratin antibodies, EMA, and MIA almost consistently stained all the tumors. CD10 and vimentin were negative in cRO and cChRCC, while mostly positive in cPRCC and TCRCC. Cathepsin K and TFE3 were invariably negative in all the evaluated cohorts. Ki67 proliferative index was low in all tumors, except for TCRCC where it was expressed in more than 17% of the cells.

Table 16. Immunohistochemical profile of the cystic variants of renal tumors

	cRO	cChRCC	cPRCC	TCRCC
AMACR	33	0	100	87
CK7	0	100	40	70
CAIX	5	0	0	43
CD117	100	100	30	6
PAX8	80	50	90	93
vimentin	5	0	100	93
cathepsin K	2	0	20	0
CD10	4	10	70	70
CAM5.2	100	70	100	100
AE1/AE3	80	50	60	100
OSCAR	100	100	100	100
TFE3	0	0	0	0
EMA	82	100	90	77
MIA	96	100	90	100
Ki67	4.9	1	6	17.93

cRO – cystic renal oncocytoma; cChRCC – cystic chromophobe carcinoma; cPRCC – cystic papillary renal cell carcinoma; TCRCC – tubulocystic renal cell carcinoma. Percentage of cases with positive staining: ○ 0-25%; ● >25-50%; ● >50-75%; ● >75%

5.6 Molecular profiles of the cystic renal tumors

Pooled molecular findings in cystic variants of the common renal tumors evaluated in this study show variable and inconsistent results. The results are summarized in Table 17. TCRCC most frequently showed gains of 7, 17, but gains of Y and X were also present. The most frequent finding in cPRCC are gains of chromosomes 7 and 17 and loss of Y. However, many other chromosomes were found to be altered. cChRCC on contrast shows only losses, among which -1p, -2q, -6, -13, -17, -21, and -X.

Table 17. Pooled results of molecular genetic analyses of the cystic renal tumor variants.

Tumor type	**Frequent genetic abnormalities**
cRO	not analyzed
TCRCC	+7,+17,+Y,+X
pRCC	+2,+3,+7,+9,+12,+13,+16,+17,+20,+21,+22 -21, -Y No changes in *VHL*, nor in LOH 3p
cChRCC	-1p, -2q, -6, -13, -17, -21, and -X

5.7 Prognostic value of tubular or cystic architecture across the RCC subtypes

To check whether cystic and tubular tumor architecture is associated with a better patient outcome, we analyzed overall survival rates across the tumor types using Kaplan Mayer survival analysis. The analysis may be limited due to the rarity of these tumors, and therefore a small number of cases, and lack of matching by age and stage. Nevertheless, it gives a good indication of whether this question needs further research and attention. Generally, the survival plots were more favorable in cystic variants of the

tumors; however, the differences were not statistically significant (Figure 14). The majority of the patients in the study, across the tumor types, were alive and well on their last follow-up examination. Several patients eventually died; however, most of them died of a condition other than kidney cancer. A small number of cases in the cohorts did not allow disease-specific survival analysis.

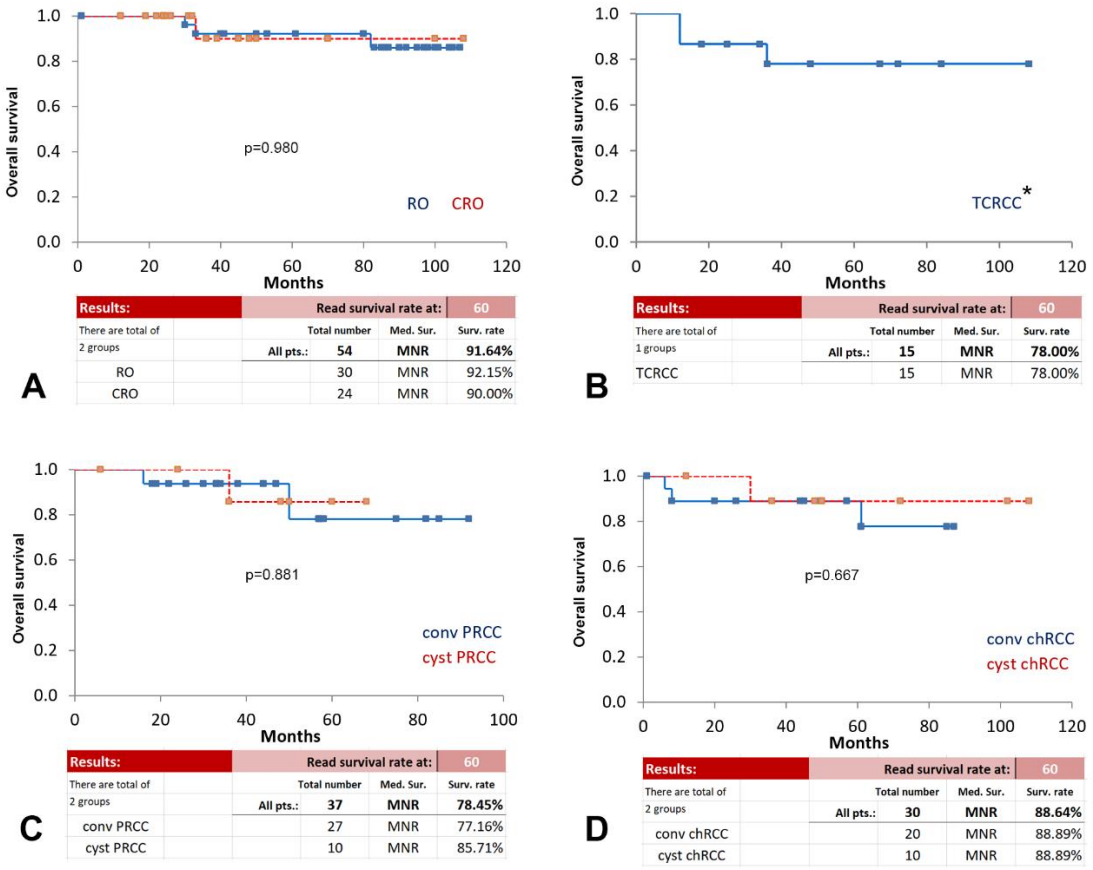

Figure 14. Kaplan Mayer survival plots of the investigated cohorts of renal tumors. (A) Cystic RO vs. conventional RO. The overall survival rates at 60 months were similar, and the difference was not significant (p=0.98). (B) Overall survival for TCRCC at 60 months (*including 4 cases that were subsequently molecularly reclassified as non-TCRCC) reveals an excellent prognosis of this tumor TRCC. (C) The overall survival rate of cystic PRCC is more favorable than conventional PRCC; however, the difference was not statistically significant (p=0.881). (D) The overall survival rate of cystic ChRCC shows a more favorable outcome for these patients at 60 months, compared to conventional ChRCC. Nevertheless, the difference was not statistically significant (p=0.667). The small number of cases due to the rarity of these tumors affected the statistical power and results.

6 DISCUSSION

Renal neoplasms are histologically heterogeneous and often present with mixed morphology, creating difficulties in the diagnostics and classification of these tumors. The same tumor type morphology may range from solid to cystic, clear cells to eosinophilic cells, low grade to high grade, with significant overlapping and mixed morphologies. In line with the morphology, the genetics of these tumors is also heterogeneous. Recently, tremendous efforts have been made in dissecting the molecular biology of the three major types of renal cell carcinoma, namely the clear cell RCC, PRCC, ChRCC (32, 33, 69).

Besides the TCRCC, a rare tumor of which less than 100 cases were reported so far, our study included small cohorts of the rare cystic or tubulocystic forms of common renal tumors collected in-house and through consultations from multiple institutions worldwide. Cystic forms of renal tumors have been rising interest over the past years as they appear to have better disease-free and overall survival than their grossly solid forms (70, 71). However, the cause and the mechanism of tubulocystic tumor growth are still unclear and whether the morphology affects the tumor behavior. In addition, do the cystic tumors differ in biomarker characteristics compared to their conventional forms, and whether the expression of common biomarkers affects the tumor aggressiveness in cystic forms.

Our investigations revealed that TCRCC has a distinct morphology, immunophenotype, and molecular-genetic features that confirm this tumor is a separate entity. Further, TCRCC is often associated with PRCC-like areas or high-grade RCC-like areas. Those cases should be carefully evaluated and the diagnosis of TCRCC excluded

if the associated areas are of high-grade solid morphology, show unusual immunophenotype or molecular genetic characteristics for TCRCC. Pure TCRCC bears an excellent prognosis when more aggressive mimickers are excluded.

A cystic form of RO represents a significant diagnostic challenge, especially on a small biopsy. This benign entity may closely represent malignant TCRCC, and those two should be correctly distinguished. Except for the architectural pattern, cystic RO is not significantly different from its solid form regarding immunohistochemistry and molecular genetic features. The outcome of this benign entity remains excellent. Cystic ChRCC is a rare and unusual morphological variant. Similar to its solid form, the cystic variant shows characteristic multiple chromosomal losses, in contrast to other renal tumors, which often show gains. Except for the cystic architecture, these tumors have a similar profile and molecular features as their solid forms, but the outcome seems to be better, although not statistically significant in this study. The same applies to the cystic form of the PRCC. The main findings of this study will be further discussed below.

RO is a benign renal neoplasm, and despite occasional vascular or fat tissue extension, hemorrhage, oncoblasts, microscopic necrosis, pleomorphic nuclei, or a few mitoses, no local recurrence, distant metastasis, or death due to tumor is reported in recent studies with a follow-up of at least five years (72). RO may mimic malignant renal tumors when solid and nested growth patterns are seen (49% to 89% cases), which are also featured in other oncocytic/eosinophilic renal tumors, such as a granular variant of clear cell RCC, ChRCC, hybrid oncocytic/chromophobe tumors, and an oncocytic variant of PRCC. Less commonly, RO presents with tubulocystic architecture (3% to 7%), a morphology that may mimic TCRCC. This study compared the morphology and immunohistochemistry of 24 cROs and 15 TCRCCs to establish the most useful features

that distinguish between these two entities. The presence of at least focal solid nests or islands of tumor cells, which were observed in all cases of cRO in this study, were much less common and quite limited in TCRCC and may also help differentiate between these tumors. The type of intervening stroma can be another helpful morphologic feature because loose stroma was regularly seen in cRO, whereas TCRCC usually contained fibrotic and more compact stromal components. In addition, no mitotic figures were found in any of the CROs, and the majority of them demonstrated lower nucleolar grades (1 or 2). In contrast, TCRCC showed focal mitotic figures in about a quarter of the cases, and nucleolar grade 3 was present in 60% of TCRCC. Microscopic necrosis was not seen in any cRO, but was found in about a third of TCRCC. The development of radiologically guided percutaneous needle biopsies, which provide small amounts of tissue or cellular material for assessing renal masses, has introduced novel diagnostic challenges for the pathologist. In such circumstances, many morphologic features may not be available for evaluation in the limited tissue, and the supplementary immunohistochemistry may help establish the diagnosis. In this study, none of the evaluated antibodies showed exclusive specificity for either cRO or TCRCC; although CD117 was highly discriminative, as all CROs were diffusely positive, whereas only 1 case of TCRCC showed weak cytoplasmic staining. We found TCRCC to be more frequently positive for vimentin, CD10, AMACR, and CK7 and had a higher proliferative index by Ki-67 (> 15%). Vimentin was very useful, as it was either negative or scattered cell positive in cRO, in contrast to TCRCC, in which it was strongly and diffusely expressed (42). Our study results are in concordance with the data mentioned above (half of the cRO showed scattered positivity, and more than 80% of TCRCC showed diffuse strong positivity). CD10 and AMACR were often negative in cRO, whereas diffuse or focal positivity was observed in TCRCC. cRO also

consistently expressed CK7 in isolated cells or scattered pattern, much less than observed in TCRCC. Proliferation activity in CRO was also lower (< 5% cells), whereas TCRCC demonstrated higher expression (> 15% cells). CAIX, AE1/AE3, CAM5.2, OSCAR, MIA, EMA were of limited diagnostic value. Performing additional studies for differentiation of these tumors, including genetic and molecular, may rarely be necessary, but it may be helpful in most difficult cases. Cytogenetic changes found most frequently in RO include losses of chromosome 1 or Y and balanced translocation of the 11q13 breakpoint region (72). The most frequent cytogenetic change in TCRCC includes the gain of chromosome 7, although occasionally gains of both chromosomes 7 and 17 may occur (73, 74). To conclude, cRO and TCRCC may be challenging to distinguish. However, careful morphologic assessment for the presence of solid tumor growth or islands, the type of tumor stroma, nucleolar grade, mitotic activity, and necrosis, and aided by a limited immunopanel that includes vimentin, CD10, CD117, AMACR, CK7, and Ki-67, will lead to establishing a correct diagnosis.

TC-RCC is a rare tumor with ultrastructural and immunohistochemical results showing mixed features of proximal and distal tubules (73, 75). Gains of chromosomes 7 or 17 are characteristic of TC-RCC (76, 77). About 100 cases of TC-RCC are published previously, with a few studies suggesting a relationship between TC-RCC and PRCC (45). Nevertheless, no discriminating immunohistochemical markers exist, and the immunoprofiles of TCRCC and PRCC are similar. AMACR is usually diffusely and strongly positive in both TCRCC and PRCC. Other markers, including PAX-2, CD10, 34bE12, cytokeratin 19, and cytokeratin 7, were evaluated in the previous studies and showed limited usefulness in establishing a correct diagnosis in complicated cases (74, 77). Our cohort consisted of 15 cases with a tubulocystic pattern, including 7 with foci of

PRCC-like features and 1 with PRCC/RAT-like features. Another two cases had small areas of high-grade RCC NOS. We analyzed separately distinct histologic components. FISH analysis of chromosomes 7, 17, and Y was variable. The majority of cases showed disomy of chromosome 7, whereas half of the cases showed polysomy or gain of chromosome 17, and in one case, there was a loss of the Y chromosome in the TCRCC area. Three of 7 possible cases with PRCC components were suitable for molecular analysis and revealed different profiles than TCRCC component. All three cases showed polysomies of chromosome 17, and one showed polysomy of chromosome 7. In one case, polysomy of chromosome X (XXY) was found. The case, which has later proven to be HLRCC, showed polysomy of 7, 17, and Y in TCRCC-like areas and disomy of 7 and polysomy of 17 with disomy of Y in PRCC-like areas. In a recent study, a unique molecular signature of TCRCC was reported using comparative genomic microarray analysis (74). TCRCC showed gains of chromosome 17 but not chromosome 7, whereas most PRCCs show gains in both chromosomes 7 and 17. A recent study by Zhou et al. included 12 cases of TCRCC, of which 10/12 had a chromosome 7 gain, 8/12 had a chromosome 17 gain, and 8/9 cases had a loss of Y. The authors concluded that these tumors are closely related entities (45). However, the pattern of chromosomal abnormalities present in our cases showed the heterogenic nature of TCRCC even within a single tumorous lesion.

Moreover, gains of chromosomes 7 and 17 were found only in one case with areas morphologically resembling PRCC. Our FISH analysis raised the question of whether PRCC-like areas are part of morphologic heterogeneity or represent differentiation toward PRCC. Unfortunately, the number of analyzable cases in our study was limited, and we could not elucidate this phenomenon further. We further analyzed

three cases with an aggressive form of TCRCC in patients under 45 years of age for possible *FH* gene mutation. One of the cases with a predominantly tubulocystic pattern (95%) and only a small area of papillary architecture (5%), was positive for *FH* gene mutation. Genetic heterogeneity and unfavorable outcomes in 3 of 9 patients with heterogenous tumor raise questions about diagnosing TC-RCC in cases with heterogeneous histologic patterns. Our analysis revealed that TCRCC has variable chromosome 7 and 17 status. Recently, a possible relationship between TCRCC and collecting duct carcinoma (CDC) has been revisited (78, 79); however, a distinct immunohistochemical profile was reported in a different study with TCRCC overexpressing vimentin, p53, and AMACR compared to CDC (80). Our data strongly suggest that TCRCC with a heterogeneous component should not be diagnosed as such and may have an adverse outcome. For cases with heterogeneous components, unclassified RCC may be a better diagnostic category. Hereditary leiomyomatosis-related RCC can be morphologically indistinguishable from "high-grade" TC-RCC; therefore, in TCRCC cases with high-grade features, the status of the *FH* gene should be tested.

Type 1 PRCC is currently considered a distinct entity with defined histologic and immunohistochemical features and typical molecular-genetic profile. Our small cohort consisted of a homogenous subset of type 1 PRCC with large unilocular cystic necrotic tumors encapsulated by thick fibrous tissue, morphologically, immunohistochemically, and genetically consistent with PRCC type 1. Tumor necrosis represents an interesting parameter in the assessment of prognosis, owing to its easy and reproducible identification in the routine histopathologic examination. However, conflicting results have been published to date, as there are no uniformly established criteria (81, 82). Although tumor necrosis is often reported as an adverse prognostic

factor, its significance is only well established in clear cell RCC (83, 84). A recently proposed grading system for clear cell RCC considers only coagulative-type necrosis as a significant prognostic marker. No such criteria have been established for PRCC. In coagulative type necrosis architecture with neoplastic cells showing no nuclei and with minor structural damage is preserved, giving the appearance of so-called “ghost cells.” On the contrary, in liquefactive necrosis, dead cells are digested, resulting in the transformation of the tissue into a liquid, viscous mass. In our cohort, the necrosis was of a liquefactive type, as large parts of the tumors were altered into a liquid thick, largely hemorrhagic mass. None of the tumors demonstrated aggressive behavior in our series of 10, mostly necrotic PRCC type 1.

ChRCC represents approximately 5% of all renal cell carcinomas. Two morphological variants are traditionally recognized: the classical and the eosinophilic variant (85). In addition, several variants have been described. We carefully selected a cohort of ChRCC with large cystic spaces, slightly irregular in shape and size, and three cases of similar tumors but with compressed cystic and tubular spaces, resulting in a growth pattern with slit-like spaces. The raisinoid nuclei with perinuclear clearing (halo) were present in all the cases. Our cases were positive for PAX8, MIA, CD117, CK 7, EMA, and OSCAR with low Ki67 proliferation index in all cases, showing a similar immunophenotype to that of conventional ChRCC (86). Five of our cases were suitable for aCGH analysis, revealing multiple losses of chromosomes 1p, 2q, 6, 13, 17, 21, and X in two cases, while the remaining three cases showed no numerical chromosomal aberrations. Nevertheless, cases of ChRCC with normal chromosomal status have been reported previously (87).

The following renal cell lesions should be considered in the differential diagnosis of cChRCC the following diagnoses should be considered: cystic/multicystic variant of renal oncocytoma, multilocular cystic clear cell carcinoma/neoplasm of low malignant potential (MCCCC), granular/eosinophilic high-grade variant of clear cell RCC, TCRCC, and mixed epithelial stromal tumor (MEST)/cystic nephroma (CN). The Kaplan Mayer curve showed a somewhat better outcome for the patients in the cChRCC group; nevertheless, the differences were not statistically significant. A low number of cases may be one reason for the low statistical power of the test, and the results should be validated in a more extensive series.

6.1 Limitations of the study

Our study investigates rare morphologic variants of several types of conventional renal lesions, as well as one recently recognized entity with a similar architectural pattern. Although the number of cases in our cohorts is small, important morphological, immunohistochemical and molecular genetic results were retrieved. However, a small number of cases may be a limiting factor, and caution is required to interpret and generalize the results. Future studies on larger cohorts will eventually validate the results.

7 CONCLUSIONS

We characterized morphological features, immunoprofile, and molecular genetic features of the newly established kidney tumor, the TCRCC. In addition, we characterized highly unusual tubulocystic/cystic forms of the RO, ChRCC, PRCC and compared them with their conventional counterparts.

1. TCRCC is a distinct kidney tumor with defined morphology, but currently, none of the immunohistochemical and molecular biomarkers are strictly specific for this tumor. A combination of morphological and immunohistochemical features should be informative in most cases.
2. The presence of associated high-grade tumor areas in TCRCC necessitates careful evaluation and exclusion of more aggressive tumor types, often requiring molecular-genetic analysis. However, with the exclusion of the non-pure TCRCC cases, this entity has an excellent prognosis, based on the data on a limited number of cases.
3. Cystic variants of RO, ChRCC, and PRCC have similar immunohistochemical properties and molecular features compared to their conventional variants.
4. Cystic and tubulocystic morphology indicates better outcomes compared to conventional solid variants. However, the differences between the variants were not statistically significant and require validation on larger cohorts.
5. AMACR, CK7, CAIX, CD117, Vimentin, CD10, and Ki67 immunohistochemistry, combined with morphological features, may be

sufficient to differentiate most of the cases of cystic and conventional variants of RO, TCRCC, PRCC, and ChRCC.

6. Molecular genetic alterations in renal tumors are heterogeneous, ranging from none detectable to multiple chromosomal gains or losses. Nevertheless, the genetic pattern of PRCC type 1 and ChRCC is more distinguishable and may help diagnostic decisions in complex cases. In addition, defined molecular genetic properties may provide therapeutic guidance.

8 SUMMARY

Renal tumors are a heterogeneous group of neoplasms recently subjected to intensive research, resulting in several new entities and reclassification. Therefore, we aimed to characterize the morphological features, immunoprofile, and molecular genetic profile of a new entity, namely the tubulocystic renal cell carcinoma. Additionally, we aimed to characterize tubulocystic/cystic variants of selected common renal tumor subtypes and determine the most useful properties for the differentiation of these tumors in diagnostic practice. Finally, we aimed to evaluate the effect of tubulocystic histological pattern on the patients' survival.

We selected 24 renal oncocytomas (RO), 10 papillary renal cell carcinomas (PRCC), 10 chromophobe renal carcinomas (ChRCC), and 15 tubulocystic renal cell carcinomas (TCRCC) with a predominantly (more than 50%) cystic architecture and compared them with a control cohort of their conventional counterparts. We used light microscopy, immunohistochemistry, array comparative genomic hybridization, PCR, and Sanger sequencing to evaluate the tumors for morphology, immunophenotype, chromosomal aberrations, and mutational analyses.

Tubulocystic renal cell carcinoma showed distinctive pathological and molecular characteristics and is a separate tumor entity. Nevertheless, 5/11 TCRCC cases were associated with PRCC-like, high grade or CCPRCC/RAT-like areas, and cases with high grade or RAT-like morphology showed less favorable outcomes. Immunohistochemically, TCRCC showed diffuse staining for CAM5.2, MIA, OSCAR; vimentin and AMACR mainly were positive; EMA and CA-IX showed variable positivity; CD117 was negative in 93.3% of cases, and average Ki-67 proliferative index

was 17.93. Gain of chromosomes 7, 17 and Y was present but not consistently found across the cases. Cystic variants of RO, PRCC, ChRCC show similar immunophenotype and molecular genetic characteristics compared to their conventional counterparts. The most valuable antibodies in diagnosing cystic renal tumors are AMACR, CK7, CAIX, CD117, Vimentin, CD10, and Ki67 in combination with tumor morphology. Overall survival plots of Cystic RO vs. conventional RO at 60 months were similar, and the difference was not significant (p=0.98). Overall survival for TCRCC at 60 months reveals an excellent prognosis of this tumor TRCC. The overall survival rate of cystic PRCC is more favorable than conventional PRCC; however, the difference was not statistically significant (p=0.881). The overall survival rate of cystic ChRCC shows a more favorable outcome for these patients compared to conventional ChRCC, but the difference was not statistically significant (p=0.667). Molecular genetic alterations in renal tumors are heterogeneous, ranging from none detected to multiple chromosomal gains or losses.

KEYWORDS: tubulocystic renal cell carcinoma, renal oncocytoma, papillary renal cell carcinoma, chromophobe renal cell carcinoma, immunophenotype, chromosomal aberrations, outcome, cystic variants

9 SAŽETAK

Kliničko-patološka i molekularna karakterizacija tubulocističnih varijanti tumora bubrega

Faruk Skenderi, Zagreb 2021

Bubrežni tumori heterogena su skupina novotvorina koje su odnedavno intenzivno istraživane, što je rezultiralo s nekoliko novih entiteta i promjenom klasifikacije. Stoga, naš cilj je bio karakterizirati morfološke značajke, imunoprofil i molekularno-genetski profil novog entiteta, tubulocističnog karcinoma bubrežnih stanica. Pored toga, htjeli smo karakterizirati tubulocistične/cistične varijante odabranih uobičajenih podtipova tumora bubrega i odrediti najkorisnija svojstva za diferencijaciju ovih tumora u dijagnostičkoj praksi. Konačno, imali smo za cilj procijeniti učinak tubulocističnog histološkog obrasca na preživljavanje pacijenata.

Odabrali smo 24 bubrežna onkocitoma (RO), 10 papilarnih karcinoma bubrežnih stanica (PRCC), 10 kromofobnih karcinoma bubrega (ChRCC) i 15 tubulocističnih karcinoma bubrežnih stanica (TCRCC) s pretežno (više od 50%) cističnom arhitekturom i usporedili ih s kontrolnim kohortama njihovih konvencionalnih varijanti. Koristili smo svjetlosnu mikroskopiju, imunohistokemiju, usporednu genomsku hibridizaciju, PCR i Sanger sekvenciranje za analizu morfologije, imunofenotipa, kromosomskih aberacija i mutacijskih analiza.

Tubulocistični karcinom bubrega pokazao je prepoznatljive patološke i molekularne karakteristike i zaseban je tumorski entitet. Ipak, 5/11 slučajeva TCRCC sadržavalo je područja nalik PRCC-u, visokog stupnja ili CCPRCC-u /RAT-u, a slučajevi

s morfologijom visokog stupnja ili RAT-u pokazali su lošiji ishod. Imunohistokemijski, TCRCC je pokazao difuzno bojenje na CAM5.2, MIA, OSCAR; vimentin i AMACR bili su uglavnom pozitivni; EMA i CA-IX pokazali su promjenjivu pozitivnost; CD117 je bio negativan u 93,3% slučajeva, a prosječni indeks proliferacije Ki-67 bio je 17,93. Višak kromosoma 7, 17 i Y je bio prisutan, ali nije dosljedno nađen u svim slučajevima. Cistične inačice RO, PRCC, ChRCC pokazuju slične imunofenotipske i molekularno-genetske značajke u usporedbi s njihovim konvencionalnim varijantama. Najkorisnija protutijela u dijagnosticiranju cističnih bubrežnih tumora su AMACR, CK7, CAIX, CD117, Vimentin, CD10 i Ki67 u kombinaciji s morfologijom tumora. Krivulje ukupnog preživljenja kod cističnog RO u odnosu na konvencionalni RO nakon 60 mjeseci su bile slične i razlika nije bila značajna (p = 0,98). Krivulje ukupnog preživljenja kod TCRCC-a nakon 60 mjeseci pokazuju izvrsnu prognozu kod ovog tumora. Ukupna stopa preživljenja kod cističnog PRCC bolja je u odnosu na konvencionalni PRCC; međutim, razlika nije bila statistički značajna (p=0,881). Ukupna stopa preživljenja kod cističnog ChRCC-a pokazuje povoljniji ishod za ove bolesnike u usporedbi s konvencionalnim ChRCC-om, ali razlika nije bila statistički značajna (p=0,667). Molekularno genetske promjene u bubrežnim tumorima su heterogene, u rasponu od nijedne otkrivene do višestrukih kromosomskih dobitaka ili gubitaka.

KLJUČNE RIJEČI: tubulocistični karcinom bubrega, bubrežni onkocitom, papilarni karcinom bubrega, kromofobni karcinom bubrega, imunofenotip, kromosomske aberacije, ishod, cistične varijante

10 REFERENCES

1. Mills SE. Histology for Pathologists: Wolters Kluwer Health; 2012.
2. Mescher AL, Junqueira LCU. Junqueira's Basic Histology: Text and Atlas: McGraw-Hill Medical; 2013.
3. Cui D, Cui D, Daley WP, Naftel JP, Haines DE, Lynch JC. Atlas of Histology: With Functional and Clinical Correlations: Wolters Kluwer Health/Lippincott Williams & Wilkins; 2011.
4. Escudier B, Porta C, Schmidinger M, Rioux-Leclercq N, Bex A, Khoo V, et al. Renal cell carcinoma: ESMO Clinical Practice Guidelines for diagnosis, treatment and follow-up. Ann Oncol. 2016;27(suppl 5):v58-v68.
5. Siegel RL, Miller KD, Jemal A. Cancer statistics, 2016. CA Cancer J Clin. 2016;66(1):7-30.
6. Scelo G, Larose TL. Epidemiology and Risk Factors for Kidney Cancer. J Clin Oncol. 2018 Oct 29;36(36):JCO2018791905.
7. Moch H, Cubilla AL, Humphrey PA, Reuter VE, Ulbright TM. The 2016 WHO Classification of Tumours of the Urinary System and Male Genital Organs-Part A: Renal, Penile, and Testicular Tumours. Eur Urol. 2016 Jul;70(1):93-105.
8. Miller KD, Siegel RL, Lin CC, Mariotto AB, Kramer JL, Rowland JH, et al. Cancer treatment and survivorship statistics, 2016. CA Cancer J Clin. 2016 Jul;66(4):271-89.
9. Hollingsworth JM, Miller DC, Daignault S, Hollenbeck BK. Rising incidence of small renal masses: a need to reassess treatment effect. J Natl Cancer Inst. 2006;98(18):1331-4.
10. Cumberbatch MG, Rota M, Catto JW, La Vecchia C. The Role of Tobacco Smoke in Bladder and Kidney Carcinogenesis: A Comparison of Exposures and Meta-analysis of Incidence and Mortality Risks. Eur Urol. 2016;70(3):458-66.
11. Moch H, Humphrey PA, Ulbright TM, Reuter VE (ed.). World Health Organization classification of tumours of the urinary system and male genital organs. 4th ed. Lyon, France: IARC Press; 2016.

12. Brennan JF, Stilmant MM, Babayan RK, Siroky MB. Acquired renal cystic disease: implications for the urologist. Br J Urol. 1991;67(4):342-8.
13. Gnarra JR, Glenn GM, Latif F, Anglard P, Lerman MI, Zbar B, et al. Molecular genetic studies of sporadic and familial renal cell carcinoma. Urol Clin North Am. 1993;20(2):207-16.
14. Argani P, Lae M, Ballard ET, Amin M, Manivel C, Hutchinson B, et al. Translocation carcinomas of the kidney after chemotherapy in childhood. J Clin Oncol. 2006;24(10):1529-34.
15. Gonzalez HC, Lamerato L, Rogers CG, Gordon SC. Chronic hepatitis C infection as a risk factor for renal cell carcinoma. Dig Dis Sci. 2015;60(6):1820-4.
16. Cheungpasitporn W, Thongprayoon C, O'Corragain OA, Edmonds PJ, Ungprasert P, Kittanamongkolchai W, Erickson SB. The risk of kidney cancer in patients with kidney stones: a systematic review and meta-analysis. QJM. 2015 Mar;108(3):205-12.
17. Williamson SR, Gill AJ, Argani P, Chen YB, Egevad L, Kristiansen G, et al. Report From the International Society of Urological Pathology (ISUP) Consultation Conference on Molecular Pathology of Urogenital Cancers: III: Molecular Pathology of Kidney Cancer. Am J Surg Pathol. 2020;44(7):e47-e65.
18. Delahunt B, Eble JN. History of the development of the classification of renal cell neoplasia. Clin Lab Med. 2005 Jun;25(2):231-46, v.
19. Montironi R, Cheng L, Scarpelli M, Lopez-Beltran A. Pathology and Genetics: Tumours of the Urinary System and Male Genital System: Clinical Implications of the 4th Edition of the WHO Classification and Beyond. Eur Urol. 2016 Jul;70(1):120-123
20. Athanazio DA, Amorim LS, da Cunha IW, Leite KRM, da Paz AR, de Paula Xavier Gomes R, et al. Classification of renal cell tumors – current concepts and use of ancillary tests: recommendations of the Brazilian Society of Pathology. Surg Exp Pathol. 2021;4(1):4.
21. Srigley JR, Delahunt B, Eble JN, Egevad L, Epstein JI, Grignon D, et al. The International Society of Urological Pathology (ISUP) Vancouver Classification of Renal Neoplasia. Am J Surg Pathol. 2013 Oct;37(10):1469-89
22. Amin MB, Gupta R, Ondrej H, McKenney JK, Michal M, Young AN, et al. Primary thyroid-like follicular carcinoma of the kidney: report of 6 cases of a

histologically distinctive adult renal epithelial neoplasm. Am J Surg Pathol. 2009 Mar;33(3):393-400.

23. Petersson F, Martinek P, Vanecek T, Pivovarcikova K, Peckova K, Ondic O, et al. Renal Cell Carcinoma With Leiomyomatous Stroma: A Group of Tumors With Indistinguishable Histopathologic Features, But 2 Distinct Genetic Profiles: Next-Generation Sequencing Analysis of 6 Cases Negative for Aberrations Related to the VHL gene. Appl Immunohistochem Mol Morphol. 2018 Mar;26(3):192-197.

24. Trpkov K, Abou-Ouf H, Hes O, Lopez JI, Nesi G, Comperat E, et al. Eosinophilic Solid and Cystic Renal Cell Carcinoma (ESC RCC): Further Morphologic and Molecular Characterization of ESC RCC as a Distinct Entity. Am J Surg Pathol. 2017;41(10):1299-308.

25. Hes O, Condom Mundo E, Peckova K, Lopez JI, Martinek P, Vanecek T, et al. Biphasic Squamoid Alveolar Renal Cell Carcinoma: A Distinctive Subtype of Papillary Renal Cell Carcinoma? Am J Surg Pathol. 2016;40(5):664-75.

26. Zhang W, Yu W, Wang Q, Jiang Y, Li Y. The clinicopathological, ultrastructural, genetic features and diagnosis of small cell variant renal oncocytoma. Acta Histochem. 2015;117(6):505-11.

27. Skenderi F, Ulamec M, Vranic S, Bilalovic N, Peckova K, Rotterova P, et al. Cystic Renal Oncocytoma and Tubulocystic Renal Cell Carcinoma: Morphologic and Immunohistochemical Comparative Study. Appl Immunohistochem Mol Morphol. 2016;24(2):112-9.

28. Hes O, Compérat EM, Rioux-Leclercq N, Kuroda N. The 2012 ISUP Vancouver and 2016 WHO classification of adult renal tumors: changes for common renal tumors. Diagn Histopath. 2016;22(2):41-6.

29. Akhtar M, Al-Bozom IA, Al Hussain T. Papillary Renal Cell Carcinoma (PRCC): An Update. Adv Anat Pathol. 2019;26(2):124-32.

30. Foix MP, Dunatov A, Martinek P, Mundó EC, Suster S, Sperga M, et al. Morphological, immunohistochemical, and chromosomal analysis of multicystic chromophobe renal cell carcinoma, an architecturally unusual challenging variant. Virchows Arch. 2016 Dec;469(6):669-678

31. Moch H, Ohashi R. Chromophobe renal cell carcinoma: current and controversial issues. Pathology. 2021 Jan;53(1):101-108.

32. Davis CF, Ricketts CJ, Wang M, Yang L, Cherniack AD, Shen H, et al. The somatic genomic landscape of chromophobe renal cell carcinoma. Cancer Cell. 2014;26(3):319-30.
33. Ricketts CJ, De Cubas AA, Fan H, Smith CC, Lang M, Reznik E, et al. The Cancer Genome Atlas Comprehensive Molecular Characterization of Renal Cell Carcinoma. Cell Rep. 2018;23(12):3698.
34. Saad AM, Gad MM, Al-Husseini MJ, Ruhban IA, Sonbol MB, Ho TH. Trends in Renal-Cell Carcinoma Incidence and Mortality in the United States in the Last 2 Decades: A SEER-Based Study. Clin Genitourin Cancer. 2019;17(1):46-57 e5.
35. Amin MB, Edge SB, Greene FL, Byrd DR, Brookland RK, Washington MK, et al. AJCC Cancer Staging Manual: Springer International Publishing; 2018.
36. Leibovich BC, Lohse CM, Crispen PL, Boorjian SA, Thompson RH, Blute ML, et al. Histological subtype is an independent predictor of outcome for patients with renal cell carcinoma. J Urol. 2010;183(4):1309-15.
37. Golshayan AR, George S, Heng DY, Elson P, Wood LS, Mekhail TM, et al. Metastatic sarcomatoid renal cell carcinoma treated with vascular endothelial growth factor-targeted therapy. J Clin Oncol. 2009;27(2):235-41.
38. Tsui KH, Shvarts O, Smith RB, Figlin RA, deKernion JB, Belldegrun A. Prognostic indicators for renal cell carcinoma: a multivariate analysis of 643 patients using the revised 1997 TNM staging criteria. J Urol. 2000;163(4):1090-5; quiz 295.
39. Ficarra V, Novara G, Galfano A, Brunelli M, Cavalleri S, Martignoni G, et al. The 'Stage, Size, Grade and Necrosis' score is more accurate than the University of California Los Angeles Integrated Staging System for predicting cancer-specific survival in patients with clear cell renal cell carcinoma. BJU Int. 2009 Jan;103(2):165-70.
40. Zisman A, Pantuck AJ, Dorey F, Said JW, Shvarts O, Quintana D, et al. Improved prognostication of renal cell carcinoma using an integrated staging system. J Clin Oncol. 2001 Mar 15;19(6):1649-57.
41. Motzer RJ, Ravaud A, Patard JJ, Pandha HS, George DJ, Patel A, et al. Adjuvant Sunitinib for High-risk Renal Cell Carcinoma After Nephrectomy: Subgroup Analyses and Updated Overall Survival Results. Eur Urol. 2018;73(1):62-8.

42. Alexiev BA, Drachenberg CB. Tubulocystic carcinoma of the kidney: a histologic, immunohistochemical, and ultrastructural study. Virchows Arch. 2013 May;462(5):575-81.

43. Ulamec M, Skenderi F, Zhou M, Kruslin B, Martinek P, Grossmann P, et al. Molecular Genetic Alterations in Renal Cell Carcinomas With Tubulocystic Pattern: Tubulocystic Renal Cell Carcinoma, Tubulocystic Renal Cell Carcinoma With Heterogenous Component and Familial Leiomyomatosis-associated Renal Cell Carcinoma. Clinicopathologic and Molecular Genetic Analysis of 15 Cases. Appl Immunohistochem Mol Morphol. 2016;24(7):521-30.

44. Deshmukh M, Shet T, Bakshi G, Desai S. Tubulocystic carcinoma of kidney associated with papillary renal cell carcinoma. Indian J Pathol Microbiol. 2011 Jan-Mar;54(1):127-30.

45. Zhou M, Yang XJ, Lopez JI, Shah RB, Hes O, Shen SS, et al. Renal tubulocystic carcinoma is closely related to papillary renal cell carcinoma: implications for pathologic classification. Am J Surg Pathol. 2009 Dec;33(12):1840-9.

46. Bhullar JS, Thamboo T, Esuvaranathan K. Unique case of tubulocystic carcinoma of the kidney with sarcomatoid features: a new entity. Urology. 2011;78(5):1071-2.

47. Tran T, Jones CL, Williamson SR, Eble JN, Grignon DJ, Zhang S, et al. Tubulocystic renal cell carcinoma is an entity that is immunohistochemically and genetically distinct from papillary renal cell carcinoma. Histopathology. 2016 May;68(6):850-7.

48. Lawrie CH, Armesto M, Fernandez-Mercado M, Arestín M, Manterola L, Goicoechea I, et al. Noncoding RNA Expression and Targeted Next-Generation Sequencing Distinguish Tubulocystic Renal Cell Carcinoma (TC-RCC) from Other Renal Neoplasms. J Mol Diagn. 2018 Jan;20(1):34-45.

49. Sarungbam J, Mehra R, Tomlins SA, Smith SC, Jayakumaran G, Al-Ahmadie H, et al. Tubulocystic renal cell carcinoma: a distinct clinicopathologic entity with a characteristic genomic profile. Mod Pathol. 2019;32(5):701-9.

50. Kuroda N, Tamura M, Hes O, Michal M, Gatalica Z. Chromophobe renal cell carcinoma with neuroendocrine differentiation and sarcomatoid change. Pathol Int. 2011 Sep;61(9):552-4.

51. Dundr P, Pesl M, Povýsil C, Tvrdík D, Pavlík I, Soukup V, Dvorácek J. Pigmented microcystic chromophobe renal cell carcinoma. Pathol Res Pract. 2007;203(8):593-7.
52. Kuroda N, Iiyama T, Moriki T, Shuin T, Enzan H. Chromophobe renal cell carcinoma with focal papillary configuration, nuclear basaloid arrangement and stromal osseous metaplasia containing fatty bone marrow element. Histopathology. 2005;46(6):712-3.
53. Skenderi F, Ulamec M, Vanecek T, Martinek P, Alaghehbandan R, Foix MP, et al. Warthin-like papillary renal cell carcinoma: Clinicopathologic, morphologic, immunohistochemical and molecular genetic analysis of 11 cases. Ann Diagn Pathol. 2017 Apr;27:48-56.
54. Ulamec M, Skenderi F, Trpkov K, Kruslin B, Vranic S, Bulimbasic S, et al. Solid papillary renal cell carcinoma: clinicopathologic, morphologic, and immunohistochemical analysis of 10 cases and review of the literature. Ann Diagn Pathol. 2016;23:51-7.
55. Honda Y, Goto K, Nakamura Y, Terada H, Sentani K, Yasui W, et al. Imaging features of papillary renal cell carcinoma with cystic change-dominant appearance in the era of the 2016 WHO classification. Abdom Radiol (NY). 2017 Jul;42(7):1850-1856.
56. Peckova K, Martinek P, Pivovarcikova K, Vanecek T, Alaghehbandan R, Prochazkova K, et al. Cystic and necrotic papillary renal cell carcinoma: prognosis, morphology, immunohistochemical, and molecular-genetic profile of 10 cases. Ann Diagn Pathol. 2017 Feb;26:23-30.
57. Kim SH, Park B, Joo J, Joung JY, Seo HK, Lee KH, et al. Retrospective analysis of 25 immunohistochemical tissue markers for differentiating multilocular cystic renal neoplasm of low malignant potential and multicystic renal cell carcinoma. Histol Histopathol. 2018 Jun;33(6):589-596.
58. Huber J, Winkler A, Jakobi H, Bruckner T, Roth W, Hallscheidt P, et al. Preoperative decision making for renal cell carcinoma: cystic morphology in cross-sectional imaging might predict lower malignant potential. Urol Oncol. 2014 Jan;32(1):37.e1-6.
59. Donin NM, Mohan S, Pham H, Chandarana H, Doshi A, Deng FM, et al. Clinicopathologic outcomes of cystic renal cell carcinoma. Clin Genitourin Cancer. 2015 Feb;13(1):67-70.

60. Webster WS, Thompson RH, Cheville JC, Lohse CM, Blute ML, Leibovich BC. Surgical resection provides excellent outcomes for patients with cystic clear cell renal cell carcinoma. Urology. 2007 Nov;70(5):900-4

61. Li T, Chen J, Jiang Y, Ning X, Peng S, Wang J, et al. Multilocular Cystic Renal Cell Neoplasm of Low Malignant Potential: A Series of 76 Cases. Clin Genitourin Cancer. 2016 Dec;14(6):e553-e557.

62. Kashan M, Ghanaat M, Hötker AM, Duzgol C, Sanchez A, DiNatale RG, et al. Cystic Renal Cell Carcinoma: A Report on Outcomes of Surgery and Active Surveillance in Patients Retrospectively Identified on Pretreatment Imaging. J Urol. 2018 Aug;200(2):275-282.

63. Kuroda N, Ohe C, Mikami S, Inoue K, Nagashima Y, Cohen RJ, et al. Multilocular cystic renal cell carcinoma with focus on clinical and pathobiological aspects. Histol Histopathol. 2012 Aug;27(8):969-74.

64. Massari F, Ciccarese C, Hes O, Michal M, Caliò A, Fiorentino M, et al. The Tumor Entity Denominated "clear cell-papillary renal cell carcinoma" According to the WHO 2016 new Classification, have the Clinical Characters of a Renal Cell Adenoma as does Harbor a Benign Outcome. Pathol Oncol Res. 2018 Jul;24(3):447-456.

65. Kryvenko ON. Do clear cell papillary renal cell carcinomas have malignant potential? Diolombi ML, Cheng L, Argani P, Epstein JI.Am J Surg Pathol. December 2015;39(12):1621-1634. Urol Oncol. 2017 Jun;35(6):451-452.

66. Delahunt B, Eble JN, Egevad L, Samaratunga H. Grading of renal cell carcinoma. Histopathology. 2019 Jan;74(1):4-17

67. Herman JG, Graff JR, Myöhänen S, Nelkin BD, Baylin SB. Methylation-specific PCR: a novel PCR assay for methylation status of CpG islands. Proc Natl Acad Sci USA. 1996 Sep 3;93(18):9821-6.

68. Cancer Genome Atlas Research N, Linehan WM, Spellman PT, Ricketts CJ, Creighton CJ, Fei SS, et al. Comprehensive Molecular Characterization of Papillary Renal-Cell Carcinoma. N Engl J Med. 2016;374(2):135-45.

69. Linehan WM, Ricketts CJ. The Cancer Genome Atlas of renal cell carcinoma: findings and clinical implications. Nat Rev Urol. 2019;16(9):539-52.

70. Paner GP, Cimadamore A, Darrell CM, Tretiakova MS, Montironi R. Surgical pathology of cystic renal cell carcinomas: is there an overestimation of malignancy? Diagn Histopath. 2020;26(7):320-9.

71. Jhaveri K, Gupta P, Elmi A, Flor L, Moshonov H, Evans A, Jewett M. Cystic renal cell carcinomas: do they grow, metastasize, or recur? AJR Am J Roentgenol. 2013 Aug;201(2):W292-6.

72. Trpkov K, Yilmaz A, Uzer D, Dishongh KM, Quick CM, Bismar TA, et al. Renal oncocytoma revisited: a clinicopathological study of 109 cases with emphasis on problematic diagnostic features. Histopathology. 2010;57(6):893-906.

73. Kuroda N, Matsumoto H, Ohe C, Mikami S, Nagashima Y, Inoue K, et al. Review of tubulocystic carcinoma of the kidney with focus on clinical and pathobiological aspects. Pol J Pathol. 2013;64(4):233-7.

74. Yang XJ, Zhou M, Hes O, Shen S, Li R, Lopez J, et al. Tubulocystic carcinoma of the kidney: clinicopathologic and molecular characterization. Am J Surg Pathol. 2008;32(2):177-87.

75. Kong MX, Hale C, Subietas-Mayol A, Lee P, Cassai ND, McRae G, et al. Bilateral tubulocystic renal cell carcinomas in diabetic end-stage renal disease: first case report with cytogenetic and ultrastructural studies. Rare Tumors. 2013 Nov 7;5(4):e57.

76. Sangle NA, Mao R, Shetty S, Schiffman JD, Dechet C, Layfield L, et al. Novel molecular aberrations and pathologic findings in a tubulocystic variant of renal cell carcinoma. Indian J Pathol Microbiol. 2013;56(4):428-33.

77. Chen N, Nie L, Gong J, Chen X, Xu M, Chen M, et al. Gains of chromosomes 7 and 17 in tubulocystic carcinoma of kidney: two cases with fluorescence in situ hybridisation analysis. J Clin Pathol. 2014;67(11):1006-9.

78. Al-Hussain TO, Alahmadi B, Junejo NN, Alshammari K, Bakshi N, Alzahrani HM. Tubulocystic renal cell carcinoma with poorly differentiated foci and loss of fumarate hydratase: A case report. Urol Case Rep. 2020;33:101236.

79. Al-Hussain TO, Cheng L, Zhang S, Epstein JI. Tubulocystic carcinoma of the kidney with poorly differentiated foci: a series of 3 cases with fluorescence in situ hybridization analysis. Hum Pathol. 2013;44(7):1406-11.

80. Osunkoya AO, Young AN, Wang W, Netto GJ, Epstein JI. Comparison of gene expression profiles in tubulocystic carcinoma and collecting duct carcinoma of the kidney. Am J Surg Pathol. 2009;33(7):1103-6.

81. Leibovitch I, Lev R, Mor Y, Golomb J, Dotan ZA, Ramon J. Extensive necrosis in renal cell carcinoma specimens: potential clinical and prognostic implications. Isr Med Assoc J. 2001;3(8):563-5.

82. Zubac DP, Bostad L, Gestblom C, Kihl B, Seidal T, Wentzel-Larsen T, et al. Renal cell carcinoma: a clinicopathological follow-up study after radical nephrectomy. Scand J Urol Nephrol. 2007;41(3):191-7.

83. Delahunt B. Advances and controversies in grading and staging of renal cell carcinoma. Mod Pathol. 2009;22 Suppl 2:S24-36.

84. Delahunt B, Bethwaite PB, Nacey JN. Outcome prediction for renal cell carcinoma: evaluation of prognostic factors for tumours divided according to histological subtype. Pathology. 2007;39(5):459-65.

85. Amin MB, Paner GP, Alvarado-Cabrero I, Young AN, Stricker HJ, Lyles RH, et al. Chromophobe renal cell carcinoma: histomorphologic characteristics and evaluation of conventional pathologic prognostic parameters in 145 cases. Am J Surg Pathol. 2008;32(12):1822-34.

86. Cochand-Priollet B, Molinie V, Bougaran J, Bouvier R, Dauge-Geffroy MC, Deslignieres S, et al. Renal chromophobe cell carcinoma and oncocytoma. A comparative morphologic, histochemical, and immunohistochemical study of 124 cases. Arch Pathol Lab Med. 1997;121(10):1081-6.

87. Brunelli M, Eble JN, Zhang S, Martignoni G, Delahunt B, Cheng L. Eosinophilic and classic chromophobe renal cell carcinomas have similar frequent losses of multiple chromosomes from among chromosomes 1, 2, 6, 10, and 17, and this pattern of genetic abnormality is not present in renal oncocytoma. Mod Pathol. 2005;18(2):161-9.

11 BIOGRAPHY

Faruk Skenderi, MD, MSc was born in 1979 in Prizren, Kosovo. He graduated from the Medical Faculty in Sarajevo in 2006. After conducting scientific research at the Center for Proteomics of the Medical Faculty in Rijeka, he received his master's degree in 2011 under the mentorship of prof. Dr. Stipan Jonjić with the title of the thesis "Isolation and characterization of monoclonal antibodies specific for the m74 gene product of murine cytomegalovirus". Since 2007, he has been working at the Faculty of Medicine in Sarajevo as a teaching assistant. He has been working at the Clinical Center Sarajevo as a pathology resident from 2012-2017. He completed his specialization in 2017, since when he has been working in the same institution as a specialist pathologist.

He is the author and co-author of over 36 scientific articles published in peer-reviewed, referenced, indexed international publications, of which 28 are indexed in Current Contents (CC). He is the co-author of a book for pathology specialists entitled “Review of the Gynecological and Breast Pathology”.

His primary field of research is kidney cancer and breast cancer.